Atmospheric
Chemistry
and Physics

Kinetics of the reactions of OH with CO, NO, and NO_2 and of HO_2 with NO_2 in air at 1 atm pressure, room temperature, and tropospheric water vapour concentrations

Michael Rolletter[1], **Andreas Hofzumahaus**[1], **Anna Novelli**[1], **Andreas Wahner**[1], **and Hendrik Fuchs**[1,2]

[1]Institute of Climate and Energy Systems, ICE-3: Troposphere,
Forschungszentrum Jülich GmbH, Jülich, Germany
[2]Department of Physics, University of Cologne, Cologne, Germany

Correspondence: Andreas Hofzumahaus (a.hofzumahaus@fz-juelich.de) and Hendrik Fuchs
(h.fuchs@fz-juelich.de)

Abstract. The termolecular reactions of hydroxyl radicals (OH) with carbon monoxide (CO), nitric oxide (NO), and nitrogen dioxides (NO_2) and the termolecular reaction of hydroperoxy radicals (HO_2) with NO_2 greatly impact the atmospheric oxidation efficiency. Few studies have directly measured the pressure-dependent rate coefficients in air at 1 atm pressure and water vapour as third-body collision partners. In this work, rate coefficients were measured with a high accuracy ($< 5\%$) at 1 atm pressure, at room temperature, and in humidified air using laser flash photolysis and detection of the radical decay by laser-induced fluorescence. The rate coefficients derived in dry air are $(2.39 \pm 0.11) \times 10^{-13}\,\mathrm{cm^3\,s^{-1}}$ for the OH reaction with CO, $(7.3 \pm 0.4) \times 10^{-12}\,\mathrm{cm^3\,s^{-1}}$ for the OH reaction with NO, $(1.23 \pm 0.04) \times 10^{-11}\,\mathrm{cm^3\,s^{-1}}$ for the OH reaction with NO_2, and $(1.56 \pm 0.05) \times 10^{-12}\,\mathrm{cm^3\,s^{-1}}$ for the HO_2 reaction with NO_2. For the OH reactions with CO and NO, no dependence on water vapour was observed for the range of water partial pressures tested (3 to 22 hPa), and for NO_2, only a weak increase of 3 % was measured, in agreement with the study by Amedro et al. (2020). For the rate coefficient of HO_2 with NO_2 an enhancement of up to 25 % was observed. This can be explained by a faster rate coefficient of the reaction of the HO_2–water complex with NO_2 having a value of $(3.4 \pm 1.1) \times 10^{-12}\,\mathrm{cm^3\,s^{-1}}$.

1 Introduction

The inorganic pressure-dependent reactions of the OH radical with CO, NO, and NO_2 and of HO_2 with NO_2 link the chemistry of HO_x (the sum of OH and HO_2) and NO_x (NO and NO_2) in the atmosphere and affect largely the chemical transformation of pollutants (Newsome and Evans, 2017). The OH radical is the most important oxidant, reacting with most volatile compounds. Its reaction with pollutants initiates radical chain reactions in which HO_2 radicals are often formed and in which OH can be eventually regenerated. In the troposphere, for example, CO, which is emitted from combustion processes, is oxidised in the termolecular reac-

tion with OH.

$$\mathrm{OH + CO \rightleftharpoons HOCO^* \xrightarrow{M} HOCO} \quad \text{(R1)}$$
$$\mathrm{HOCO^* \rightarrow H + CO_2} \quad \text{(R2)}$$

M is a third-body collision partner. The reaction of OH with CO has been studied experimentally and theoretically over a wide range of temperatures and pressures because of its general importance in the planetary atmospheres of Earth and Mars (Atkinson et al., 2004; Burkholder et al., 2020).

Nitrogen oxides are mainly emitted by combustion processes and produced in the atmosphere by lightning. They play an important role in atmospheric radical chemistry in

several ways. The reactions of NO with peroxy radicals are responsible for the regeneration of OH radicals. Conversely, the reactions of OH with NO and NO$_2$ and of HO$_2$ with NO$_2$ form products that terminate the cyclic chain reactions between OH and HO$_2$ and can produce long-lived compounds that can act as radical reservoirs. In addition, the oxidation reaction of NO to NO$_2$ by peroxy radicals followed by NO$_2$ photolysis is the only relevant chemical source of tropospheric ozone (Ehhalt, 1999).

The termolecular reaction of OH with NO produces nitrous acid (HONO).

$$OH + NO + M \rightarrow HONO + M \qquad (R3)$$

HONO can be rapidly photolysed so that OH, NO, and HONO concentrations are in a photochemical equilibrium at daytime (Kleffmann et al., 2005).

The reaction of OH with NO$_2$ is a termolecular reaction leading to the formation of nitric acid (HNO$_3$) or pernitrous acid (HOONO).

$$OH + NO_2 + M \rightarrow HNO_3 + M \qquad (R4)$$
$$\rightleftharpoons HOONO + M \qquad (R5)$$

In the lower troposphere, HNO$_3$ is mainly lost by surface deposition due to its long chemical lifetime. The reaction channel leading to its formation is therefore a net loss of OH radicals and nitrogen oxides. In contrast, HOONO is thermally unstable and decomposes mainly in the boundary layer at mid-latitude temperatures so that there is no net loss of the reactants. If HOONO underwent other atmospheric reactions, its formation would be a radical and NO$_2$ sink, but such reactions have not been reported. The branching ratio between Reactions (R4) and (R5) increases with pressure and is approximately 14 % at atmospheric pressure and room temperature (Mollner et al., 2010).

Pernitric acid (HO$_2$NO$_2$), formed by the termolecular reaction of hydroperoxyl radicals (HO$_2$) and NO$_2$, can decompose thermally in the troposphere so that their concentrations are in a thermal equilibrium (Gierczak et al., 2005).

$$HO_2 + NO_2 + M \rightleftharpoons HO_2NO_2 + M \qquad (R6)$$
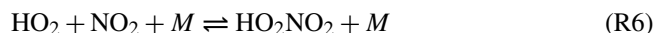
In the upper troposphere and lower stratosphere, where HO$_2$NO$_2$ is thermally stable due to the cold temperatures, its subsequent reaction with OH is an important sink for HO$_x$ radicals (Kim et al., 2007). Measurements of HO$_2$NO$_2$ can also be used to diagnose HO$_2$ and NO$_2$ concentrations, but accurate rate coefficients are required to calculate steady-state concentrations.

The reactions of OH with CO, NO, and NO$_2$ and the reaction of HO$_2$ with NO$_2$ are termolecular reactions, in which an activated association complex is formed. The rates of dissociation and collisional stabilisation of the activated complex determine the rate coefficients of the overall reaction. Therefore, the rate coefficients are pressure-dependent (expressed as the number density concentration of the bath gas

molecules, M), which can be parameterised by the Troe formalism (Troe, 1983). The Troe expression parameterises the rate using high-pressure (k_∞) and low-pressure (k_0) limiting rate coefficients. A "fall-off" transition is described by the broadening factor F. The expression used e.g. by IUPAC is (Atkinson et al., 2004)

$$k(M,T) = \frac{k_0\left(\frac{T}{300\,\text{K}}\right)^{-m} M \, k_\infty\left(\frac{T}{300\,\text{K}}\right)^{-n}}{k_0\left(\frac{T}{300\,\text{K}}\right)^{-m} M + k_\infty\left(\frac{T}{300\,\text{K}}\right)^{-n}} \, F, \qquad (1)$$

where m and n are dimensionless temperature exponents. The broadening factor F is

$$\log F = \frac{\log F_c}{1 + \left[\log\left(\frac{k_0\left(\frac{T}{300\,\text{K}}\right)^{-m} M}{k_\infty\left(\frac{T}{300\,\text{K}}\right)^{-n}}\right)/N\right]^2}, \qquad (2)$$

with $N = 0.75 - 1.27 \cdot \log F_c$ and F_c being the broadening factor at the centre of the fall-off transition. The parameterisation by NASA–JPL is only slightly different.

Despite the importance of these reactions for the atmospheric cycle of radicals and nitrogen oxides, there have only been a few studies that have directly measured their rate coefficients in air at 1 atm pressure.

The evaluations of rate coefficients are based on the limited data reported in the literature, resulting in notable differences in the values recommended by NASA–JPL (Burkholder et al., 2020) and IUPAC (Atkinson et al., 2004) at 1 atm. For example, the recommendations differ by a factor of 1.3 for the OH reaction with NO (within the stated accuracies) and by a factor of 1.8 for the HO$_2$ reaction with NO$_2$ (higher than the stated accuracies). Consequently, the predictions of atmospheric chemistry models that rely on recommendations in databases may be subject to considerable uncertainties, emphasising the need for further laboratory studies to reduce the uncertainties (Burkholder et al., 2017; Fiore et al., 2024; Ervens et al., 2024).

Previous studies have shown that the presence of water vapour can affect the rate coefficients of OH and HO$_2$ reactions through the formation of a hydrogen-bonded complex between HO$_2$ and a water molecule (Cox and Burrows, 1979; Aloisio et al., 2000; Kanno et al., 2005; Buszek et al., 2011) or by collisional stabilisation of the activated association complex by water molecules (Amedro et al., 2020; Sun et al., 2022).

For example, significantly increased rate coefficients have been observed in the self-reaction of HO$_2$ (e.g. Lii et al., 1981; Kircher and Sander, 1984) or in the reaction of HO$_2$ with NO$_2$ (Sander and Peterson, 1984) at low pressure in the presence of water vapour. However, with a few exceptions, such as the self-reaction of HO$_2$, possible water vapour dependencies have not been considered in the NASA–JPL and IUPAC recommendations due to the lack of sufficient experimental data.

In this work, a laser flash photolysis laser-induced fluorescence (LP-LIF) method was used to generate OH radicals by ozone photolysis in a flow tube and to observe the rate of their chemical decay. Unlike with many pump-and-probe instruments, the radical detection does not take place in the reaction volume but in a low-pressure cell, which allows an extremely sensitive OH fluorescence detection.

The instrument was originally developed to measure the chemical OH lifetime in ambient air at tropospheric conditions (Hofzumahaus et al., 2009; Lou et al., 2010). In atmospheric studies, the measured OH lifetime is a valuable kinetic parameter which can be used to determine the production and destruction rates of atmospheric OH, allowing the quantification of potentially unknown sources and sinks (Hofzumahaus et al., 2009; Lou et al., 2010; Kovacs and Brune, 2001; Martinez et al., 2003; Sadanaga et al., 2004a; Whalley et al., 2011; Fuchs et al., 2013, 2014; Griffith et al., 2016; Yang et al., 2016).

The inverse atmospheric OH lifetime is called the total OH reactivity (k_{OH}) and is equal to the pseudo-first-order loss rate coefficient. Its value depends on the concentrations of all atmospheric reactants i (e.g. CO, NO$_x$, hydrocarbons) and their second-order rate coefficients (k_{OH+i}).

$$k_{OH} = \sum_i k_{OH+i}[i] \tag{3}$$

In the lower troposphere, observed OH reactivity values are in the range from 1 to $100\,\text{s}^{-1}$ for conditions ranging from very clean to extremely polluted air (Hofzumahaus et al., 2009; Yang et al., 2016).

In this work, the instrument was used to determine the rate coefficients of the reaction of OH with CO, NO, and NO$_2$ and of HO$_2$ with NO$_2$ in air at atmospheric pressure and room temperature and in the presence of water vapour. Similar reactivity instruments have been used previously for kinetic studies of OH (Sadanaga et al., 2004b; Amedro et al., 2012; Nakashima et al., 2012; Stone et al., 2016; Speak et al., 2020; Berg et al., 2024; Chao et al., 2019; Sheps and Au, 2024). The method can also be used to study the kinetics of HO$_2$ radicals by adding excess CO in the flow tube to convert all initially produced OH to HO$_2$ (Nehr et al., 2011, 2012; Zhou et al., 2019). In this work, the reaction of HO$_2$ with NO$_2$ was studied using this approach.

2 Methods

2.1 Measurement of pseudo-first-order rate coefficients

The central components of the laser flash photolysis laser-induced fluorescence (LP-LIF) instrument used in this work to determine OH and HO$_2$ rate coefficients are a laminar flow tube reactor, in which OH radicals are produced by flash photolysis, and an attached fluorescence detection cell for measuring the OH decay (Fig. 1). The flow tube has a total length of 80 cm and an internal diameter of 40 mm. It is made of black anodised aluminium and is sealed at both ends by fused silica quartz windows with an antireflective coating for 266 nm (Laser Optics). The distance between the entrance of the flow tube and the sampling point of the detection cell is 50 cm. The air is replaced every 1.8 s using a mass flow controller (Bronkhorst, low Δp series, flow rate: $21\,\text{L}\,\text{min}^{-1}$) backed by a vacuum pump (Vacuubrand, MD4C). For the experiments in this work, the flow tube was kept at room temperature and ambient pressure. Sensors monitor the pressure (Honeywell, PPT), the temperature, and the relative humidity (Vaisala, HUMICAP) of the gas at the outlet of the flow tube. The flow in the flow tube is laminar with a Reynolds number of 710.

Laser flash photolysis of added ozone is used to generate excited oxygen atoms (O(^{1}D)) which react with the water molecules to form OH on a timescale of nanoseconds in the flow tube.

$$O_3 + h\nu \rightarrow O(^1D) + O_2$$

$$O(^1D) + H_2O \rightarrow 2\,OH \tag{R7}$$
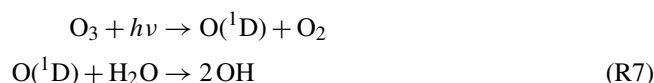
A frequency-quadrupled Nd:YAG laser (Quantel, Ultra) delivers short pulses (10 ns) of 266 nm radiation at a repetition rate of 1 Hz and pulse energies of 20 to 27 mJ. The laser beam is expanded by an optical telescope to a diameter of 30 mm. Since the collimated photolysis laser beam is not attenuated as it passes through the reaction volume (the optical density is less than 10^{-3}), the same initial OH concentration is obtained along the axis of the flow tube. Depending on the water vapour concentration and the laser pulse energy, the mean initial OH number concentrations range from 2×10^9 to $9 \times 10^9\,\text{cm}^{-3}$. To produce HO$_2$ radicals, 80 ppmv CO can be added to the gas in the flow tube for a rapid conversion of the initially produced OH. The time constant of the conversion is 2 ms.

Once formed, the OH or HO$_2$ radicals react with the reactive components in the air mixture. The concentration decreases following pseudo-first-order kinetics for all experimental conditions in this study:

$$[OH](t) = [OH]_0 \exp(-k't), \tag{4}$$

$$[HO_2](t) = [HO_2]_0 \exp(-k't), \tag{5}$$

where $[OH]_0$ and $[HO_2]_0$ are the initial radical concentrations and k' is the first-order rate coefficient of the exponential decay, which is the sum of the first-order rate coefficients of the loss in the reaction with the gaseous reactant and the wall loss.

The time-resolved decay of the radical concentration is measured in a low-pressure detection cell (3.5 hPa), which continuously draws gas from the reaction volume through a conical nozzle (Beam Dynamics, nickel, 0.6 mm orifice, $3.6\,\text{L}\,\text{min}^{-1}$ flow rate; Fig. 1). For the experiments with NO$_2$, a gold-plated nozzle was used to prevent corrosion of the inlet.
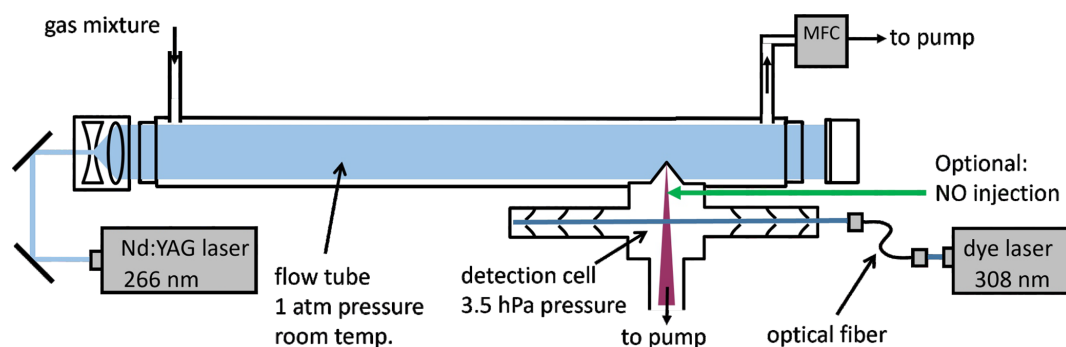
Figure 1. Schematic diagram of the instrument. The air mixture in the flow tube is exposed to laser pulses at 266 nm to generate OH radicals by flash photolysis of ozone. Air is sampled through the flow tube using a mass flow controller (MFC) backed by a pump. The decay of OH is measured by laser-induced fluorescence in a low-pressure detection cell. Optional injection of NO into the low-pressure detection cell allows the detection of HO$_2$ radicals after their chemical conversion to OH.

In the detection cell, the OH is excited by pulsed laser radiation at a wavelength of 308 nm matching the rotational absorption line Q$_1$(3) of the OH(A$^2\Sigma, v' = 0 \leftarrow$ X$^2\Pi, v'' = 0$) band transition. The UV radiation is generated by a custom-built, tunable, frequency-doubled dye laser (Strotkamp et al., 2013), which is pumped by a pulsed frequency-doubled Nd:YAG laser (Spectra-Physics, Navigator). The laser pulse repetition rate is 8.5 kHz, and the typical UV output power is 20 mW.

This system is also capable of detecting HO$_2$ if the radical is chemically converted to OH before passing through the 308 nm probing laser beam (Fig. 1). This is achieved by injecting pure NO (Air Liquide, purity 99.5 %, flow rate 5 cm^3 min^{-1} at standard conditions) into the sampled gas flow in the detection cell (Nehr et al., 2011, 2012; Miyazaki et al., 2013).

$$HO_2 + NO \rightarrow OH + NO_2 \tag{R8}$$

The added NO was purified by passing it through a cartridge filled with sodium-hydroxide-coated silica (Sigma-Aldrich, Ascarite) to avoid spurious OH background signals from the 308 nm photolysis of NO impurities. This method can give almost the same detection sensitivity (within 5 %) for HO$_2$ as for OH (Fuchs et al., 2011).

The OH fluorescence is recorded by a multi-channel scaler photon counting system (Becker & Hickl, PMS-400A) with a time resolution of 1 ms over a time period of 1 s. In this instrument, the reaction time is determined by the electronic clock of the multi-channel scaler in contrast to flow tube experiments with sliding injectors, where the reaction time is determined from the flow rate of the gas in the reaction volume. The radical detection method using OH fluorescence is extremely sensitive and allows the measurement of atmospheric OH concentrations on the order of 10^6 cm^{-3} with a measurement time of 1 min (Hofzumahaus et al., 2009; Lou et al., 2010). In the present study, in which OH reactivity is measured, typically 10 000 OH decays were averaged, resulting in an integration time for photon counting of about

1 s for each 1 ms time bin. The resulting limit of detection ($< 10^7$ cm^{-3}) made it possible to follow the decays over 2 to 3 orders of magnitude, allowing an accurate fit of the decay time.

The separation of the detection in a low-pressure cell from the high-pressure reaction volume has several advantages for the study of OH and HO$_2$ reactions at tropospheric pressures:

- The low-pressure OH detection minimises the loss of sensitivity due to quenching of the OH fluorescence, which is particularly efficient for water and O$_2$ (relative rate coefficients in units of 10^{-10} cm^3 s^{-1} at 298 K: k_{coll}(H$_2$O), k_{coll}(O$_2$), k_{coll}(N$_2$), and k_{coll}(Ar) equal 6.6, 1.4, 0.31, and 0.00036, respectively; Heard and Henderson, 2000). In contrast, previous fluorescence-based studies have often used Ar or N$_2$ as a buffer gas to reduce fluorescence quenching.

- The high detection sensitivity by the fluorescence method allows the use of low initial radical concentrations (a few 10^9 cm^{-3}) and thereby makes the influence of interfering radical–radical reactions and subsequent reactions with products including the potential photolysis of the OH reaction products by the 266 nm radiation negligible on the timescale of the measured decays.

- The method can be used to determine rate coefficients under typical tropospheric conditions of pressure and temperature and concentrations of water vapour and reactants. This is of particular interest for the study of termolecular reactions, whose rate coefficients depend on the pressure and the properties of the bath gas molecules.

- Another advantage is the minimal radical wall loss due to the slow diffusion at atmospheric pressure. This allows for the reactions to be studied on a timescale of 1 s, which is comparable to the typical timescales of HO$_x$ reactions in the lower troposphere. The timescale and

radical concentrations employed allow experiments to be carried out under pseudo-first-order conditions with lower reactant concentrations than those used in previous studies. Consequently, the impact of potentially interfering reactions of the reactants (e.g. the reaction of NO or NO$_2$ with ozone or the formation of dinitrogen tetroxide (N$_2$O$_4$) from the self-reaction of NO$_2$) is suppressed. However, unimolecular reactions, such as the reaction of an association product, may become important.

2.2 Gas mixtures

The gas mixtures overflowing the instrument inlet were prepared in two steps: first by combining flows of dry synthetic air (flow rate 23 L min^{-1}), humidified synthetic air (3 L min^{-1}), and air containing ozone (0.1 L min^{-1}). From the combined mixed flow, 1 L min^{-1} was continuously sampled by a hygrometer (Vaisala, HUMICAP) and an ozone analyser (Environment SA, O341M). The remaining flow was combined with a small flow (< 2 L min^{-1}) of a reactant gas premixed in N$_2$. All gas flows were controlled by mass flow controllers (Bronkhorst EL Flow, Bronkhorst IQ Flow, Brooks 5850). Each time, when one of the flow controller settings was changed, the flow rates were measured using a primary volumetric standard (Drycal, Definer 220), which has an accuracy of 0.75 % of the reading.

Synthetic air (79 % N$_2$ and 21 % O$_2$) was produced from evaporated high-purity liquid N$_2$ and O$_2$ (Linde, purities > 99.9999 %). Impurities in the synthetic air supply are generally below the detection limits of analytical instruments (e.g. CO < 10 ppbv, NO $+$ NO$_2$ < 10 pptv, hydrocarbons $<$ 50 pptv). Water vapour was produced by a controlled evaporation and mixing system (Bronkhorst, CEM) using pure water (Milli-Q). Ozone was produced by oxygen photolysis in synthetic air using the 185 nm radiation from a low-pressure mercury lamp. In the flow tube, typical ozone mixing ratios were 35 ppbv and the partial pressures of water vapour were in the range of 2.0 to 22.5 hPa, equivalent to relative humidities of 10 % to 98 %.

The reactant gases CO, NO, and NO$_2$ were supplied as certified mixtures in N$_2$ from commercial suppliers. The concentrations of the mixtures were controlled independently (Table 1). To measure CO concentrations, a small flow (cylinder A; Table 1) was diluted with a synthetic airflow, both controlled by mass flow controllers, and the resulting CO concentration was measured using a near-infrared cavity ring-down spectrometer (Picarro, G2401). This instrument has a high precision of a few parts per billion by volume and high linearity (Zellweger et al., 2012) and was calibrated against a CO standard from NPL (National Physical Laboratory, UK).

Two cylinders with different NO concentrations were used in this work (cylinders B and C; Table 1). For the analysis of the NO concentration in cylinder B, a flow of the gas mixture was further diluted with N$_2$ using mass flow controllers. The

resulting NO concentration was measured using a chemiluminescence instrument (Ecophysics, CLD770) for mixing ratios up to 100 ppbv. The instrument was calibrated using an NPL standard with a stated uncertainty of 0.8 %. The mixing ratios of NO and NO$_2$ in cylinders C and D (Table 1) were measured directly using a UV-VIS photometer (ABB, Limas 11HW) which is suitable for measurements up to 1000 ppmv. For all gas cylinders, the derived mixing ratios were found to be in agreement with the suppliers' specifications within the experimental uncertainties (Table 1). A weighted average of the measured and the supplier values was used to calculate the concentrations in the reaction kinetics experiments.

2.3 Kinetic analysis

The measured radical decay curves are expected to follow pseudo-first-order kinetics (Eqs. 4, 5). The corresponding time-dependent OH fluorescence signals (photon counts $N(t)$) include a constant background signal which is caused by scattered radiation from the probe laser and detector noise:

$$N(t) = N_0 \exp(-k't) + B, \qquad (6)$$

where N_0 is the initial fluorescence count and B is the background.

The parameters N_0, B, and k' were determined for the measured decay curves using a non-linear, least-square Levenberg–Marquardt fitting algorithm. The counts were weighted in the fit by their statistical errors, which follow Poisson statistics. The first 10 ms of the measured OH decay was generally discarded. The signal in this time period showed deviations from a single exponential behaviour due to inhomogeneities in the initial OH concentration, and this time was necessary for the conversion of OH to HO$_2$ in the experiments with HO$_2$.

Experiments with zero air, which contained additionally only water vapour and ozone, were performed to determine the zero rate coefficient (k_0) of the OH and HO$_2$ decays caused by wall loss and potential gas-phase reactions in the zero gas (Eq. 7). For both radicals, the values were in the range of (1.8 ± 0.1) s^{-1} for water vapour partial pressures between 2.0 and 22.5 hPa.

The calculated, known contributions to the zero rate coefficient from gas-phase reactions were very small. The reaction of the added ozone (mixing ratio 35 ppbv) with OH and HO$_2$ contributed only 0.06 and 0.0017 s^{-1}, respectively, to the reactivity. The reactivity of self-reactions of OH and HO$_2$ radicals is also less than 0.07 and 0.04 s^{-1}, respectively. The variability in the zero rate coefficient over the range of added water vapour concentrations gives an upper limit of 0.1 s^{-1} for the reactivity from potentially co-evaporated impurities of the water supply. The reactivity from potential impurities (e.g. CO, NO$_x$, hydrocarbons) in the synthetic air supply can be estimated to have an upper limit of 0.1 s^{-1}.

Table 1. Mixing ratios of the reactants in the gas mixtures as specified by the suppliers and measured in this work. All reactants were mixed in N$_2$.

Gas cylinder	Reactant	Supplier	Mix. ratio (ppmv) (supplier spec.)	Mix. ratio (ppmv) (measured)	Impurities (ppmv) (measured)
A	CO	Linde	500 ± 10	500 ± 10	–
B	NO	Air Liquide	9.96 ± 0.20	9.9 ± 0.5	–
C	NO	Air Liquide	96.3 ± 1.9	101 ± 3	$(1 \pm 3)\,NO_2$
D	NO$_2$	Praxair	520 ± 10	524 ± 3	$(2 \pm 3)\,NO$
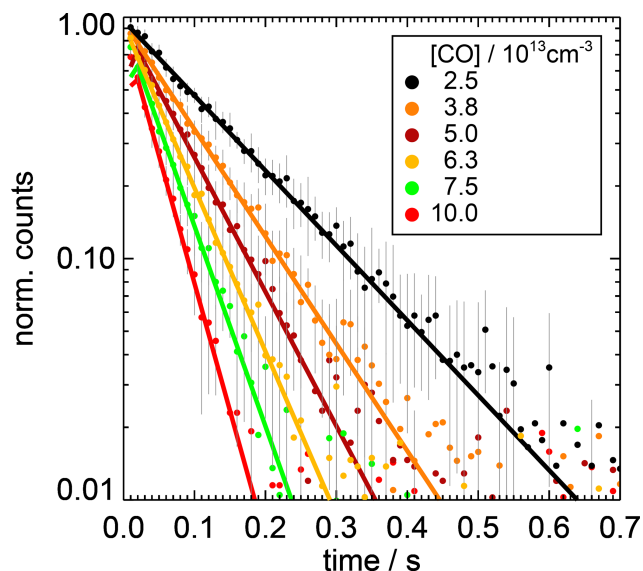
Figure 2. Examples of measured (dots) and fitted (lines) OH concentration decays (normalised to the fitted amplitude) for different CO concentrations measured at a temperature of 297 K and a pressure of 1 atm in this work. The background values determined by the fit are subtracted. For clarity, the measured decays are shown in the figure with a time resolution of 10 ms. Error bars are 1σ statistical errors in the measurements.

For these reasons, the zero rate coefficient was mainly determined by the lateral transport of radicals to the wall of the flow tube, where radicals are lost. This assumption is consistent with the diffusion of radicals, for which the mean quadratic displacement ($\langle \Delta r^2 \rangle$) can be calculated by Einstein's relation ($\langle \Delta r^2 \rangle = 4\,D\,t$, diffusion coefficients: $D(OH) = 0.217\,\text{cm}^2\text{s}^{-1}$, $D(HO_2) = 0.141\,\text{cm}^2\text{s}^{-1}$; Ivanov et al., 2007).

In the experiments, the concentrations of the reactants were varied to determine the rate coefficients (Fig. 2). The reactant concentrations gave reactivities between 0 and 40 s^{-1}. Approximately 10 decay curves, each integrating 100 to 250 photolysis laser shots, were accumulated for each reactant concentration. The slope of a linear regression of the measured first-order rate coefficients against the reactant concentration [i] gives the second-order reaction rate coefficient

k_{OH+i}. The intercept is the zero rate coefficient k_0.

$$k' = k_0 + k_{OH+i}[i] \qquad (7)$$

3 Results and discussion

3.1 Rate coefficient of the OH reaction with CO

The rate coefficient of the reaction of carbon monoxide (CO) with OH was studied in four experiments at room temperature (296 to 298 K; Table A1), in each of which the OH reactivity was measured for eight CO concentrations (Fig. 3). As CO is transparent at a wavelength of 266 nm (Okabe, 1978), effects from the photolysis of CO in the flow tube by the photolysis laser can be excluded.

The experiments differed in the water vapour content with water vapour partial pressures between 3 and 20.5 hPa equivalent to relative humidities between 13 % and 93 %. Since the rate coefficients agreed within 4 % and showed no trend with the presence of water vapour (Fig. 3), a water vapour independent value of $k_{OH+CO} = (2.38 \pm 0.11) \times 10^{-13}\,\text{cm}^3\,\text{s}^{-1}$ is determined from the weighted average of the rate coefficients determined at the different humidities (Table A1). The uncertainty is the total 2σ error, which is mainly due to the uncertainty in the CO concentration.

The reaction of OH with CO has been studied experimentally and theoretically over a wide range of conditions (e.g. Fulle et al., 1996; Atkinson et al., 2004; Johnson et al., 2014; Burkholder et al., 2020; Barker et al., 2020). It shows a complex non-Arrhenius temperature and pressure dependence. This can be explained by the formation of an activated radical intermediate, HOCO* (Smith and Zellner, 1973), which can be collisionally stabilised to HOCO or can decompose to CO$_2$ and an H atom (Reactions R1, R2).

At high temperatures (> 600 K), HOCO becomes thermally unstable and forms OH and CO (Fulle et al., 1996), while in the atmosphere (200 to 300 K) it reacts mainly with O$_2$ to form HO$_2$.

$$HOCO + O_2 \rightarrow HO_2 + CO_2 \qquad (R9)$$
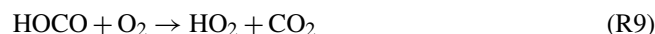
The corresponding lifetime of HOCO is 130 ns in 1 atm pressure in air at a temperature of 298 K (Miyoshi et al., 1994). Similarly, the H atom produced in the decomposition of

Table 2. Second-order rate coefficients (k) of the OH reaction with CO measured absolutely in air or N$_2$ at ambient total pressure (p) and temperature (T). In addition, recommended values by IUPAC and NASA–JPL are given for the conditions used in this work. Errors in the rate coefficients are 2σ uncertainties.

k (10^{-13} cm^3 s^{-1})	T (K)	p (hPa)	Bath gas	p(H$_2$O) (hPa)	Reference
2.18 ± 0.50[a]	298	1013	N$_2$	0.4–1.3	Paraskevopoulos and Irwin (1984)
2.30 ± 0.11[b]	298	987	N$_2$	< 0.2	Hofzumahaus and Stuhl (1984)
2.35 ± 0.20[a]	298	1013	air	0.013–27	Hynes et al. (1986)
2.44 ± 0.37[a]	298	1013	air	0–27	McCabe et al. (2001)
2.29 ± 0.28[c]	297	1017	N$_2$	–	IUPAC (Atkinson et al., 2006)
2.43 ± 0.12[c]	297	1017	air	–	NASA–JPL (Burkholder et al., 2020)
2.39 ± 0.11[b]	297 ± 1	1017 ± 8	air	3.0–20.5	this work

[a] Linear fit of measured data to ambient conditions. [b] Measurement for stated conditions. [c] Parameterisation based on the literature.

HOCO* (Reaction R2) reacts with O$_2$ to form HO$_2$ at a similar rate (Burkholder et al., 2020).

$$H + O_2 + M \rightarrow HO_2 + M \quad \text{(R10)}$$

Consistent with this mechanism, the OH decays measured in the present work showed a single exponential behaviour without regeneration of OH.

Previous experimental studies at atmospheric temperatures have shown that the OH + CO reaction (Reaction R1) does not depend on the temperature at low pressure and shows only a small decrease (about 10 %) as the temperature increases from 200 to 300 K at a pressure of 1 atm (McCabe et al., 2001; Liu and Sander, 2015). The rate coefficient has a linear pressure dependence and increases by a factor of 1.6 in the pressure range from 0 to 1 atm (Atkinson et al., 2004; Burkholder et al., 2020).

Despite its importance in atmospheric chemistry, only two absolute measurements of the rate coefficient have been reported in previous studies at room temperature and 1 atm pressure of air (Table 2; Hynes et al., 1986; McCabe et al., 2001). The data from these two studies are in very good agreement within 2 % with the results in this work. This is better than would be expected from the reported uncertainties of the pressure-dependent expressions of the rate coefficient in Hynes et al. (1986) (12 %) and in McCabe et al. (2001) (15 %) and the measurement error of 5 % in this work.

Other studies have investigated the rate coefficient in N$_2$ at ambient pressure. The values agree within 5 % to 10 % with measurements in air (Table 2). This is consistent with the experiments of Hynes et al. (1986) and McCabe et al. (2001), which show that the collisional stabilisation of the reactive complex is the same for N$_2$ and O$_2$ within the experimental uncertainties. However, experiments in N$_2$ require great care to avoid oxygen impurities, as H atoms (Reaction R2) could react not only with molecular oxygen to form HO$_2$ (Reaction R10), but also with HO$_2$, thereby regenerating OH. This can lead to an apparent reduction in the effective rate coefficient (Hofzumahaus and Stuhl, 1984; Paraskevopoulos and Irwin, 1984; Liu and Sander, 2015). Measurements in air, as

in this work, avoid this potential problem because the oxygen concentration is high and any H atoms react exclusively with O$_2$.

The results of this work are in good agreement with all previously reported absolute measurements in N$_2$ and air (Table 2) and are well within the uncertainties of recent recommendations from IUPAC (Atkinson et al., 2004) and NASA–JPL (Burkholder et al., 2020). The IUPAC-recommended value is only 5 % lower, and the NASA–JPL-recommended value is 3 % higher than the value in this work (Fig. 3). The small discrepancies suggest that the uncertainties of the recommended values are likely overestimated by a factor of 2 at atmospheric pressure, although the uncertainty over the full range of the fall-off region may be higher.

No water vapour dependence of the rate coefficient was observed. The variability in the values ((3 ± 3) %) gives an upper limit for the collisional stabilisation by water relative to air of 10. This agrees with previous measurements, where the efficiency was found to be a factor of 10 higher than that of N$_2$ at low pressures (up to 27 hPa) in pure water and helium (Paraskevopoulos and Irwin, 1984). At atmospheric pressure, however, no significant effect of water vapour on the rate coefficient could be detected for partial water vapour pressures up to 27 hPa (McCabe et al., 2001). Based on these studies and results in this work, relevant water vapour effects due to clustering of water molecules with OH as assumed in previous experimental work (Beno et al., 1985) or with HOCO as discussed in a theoretical study (Aloisio and Francisco, 2000) can be ruled out as being significant for atmospheric conditions at room temperature.

3.2 Rate coefficient of the OH reaction with NO

The rate coefficient of the OH reaction with NO (Reaction R3) was measured in air at a pressure of 1019 hPa and a temperature of 297 K. In addition, the partial pressure of water vapour was varied between 3.1 and 22.5 hPa equivalent to relative humidities between 14 % and 98 %. NO was provided by two gas standards (Table 1).
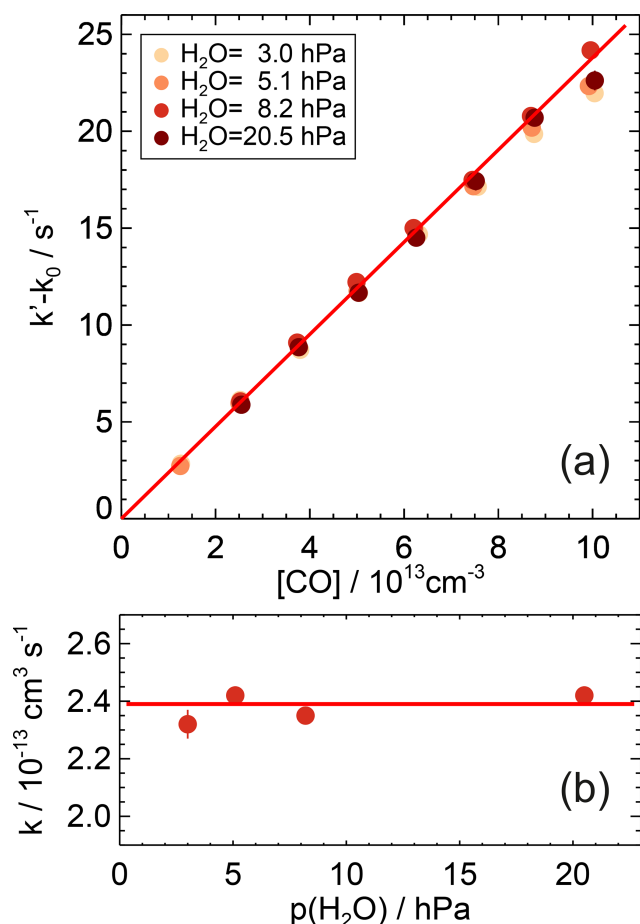
Figure 4. First-order rate coefficients of the OH reaction with NO at ambient temperature ((297 ± 1) K) and pressure ((1019 ± 3) hPa) in air and various partial pressures of water vapour. The zero rate coefficient k_0 is subtracted from the linear fit of the measured OH reactivity (Eq. 7). The slope of the red line is the weighted average of the second-order rate coefficients determined at the different humidities, as there is no observed dependence of the rate coefficient on water vapour. Error bars (1σ statistical errors) are partly smaller than the size of the symbols.

Figure 3. First-order rate coefficients of the OH reaction with CO at room temperature ((297 ± 1) K) and ambient pressure ((1017 ± 8) hPa) in air and partial water vapour pressures between 3 and 20.5 hPa (**a**). The zero rate coefficient k_0 is subtracted from the linear fit of the measured OH reactivity (Eq. 7). The slope of the red line is the weighted average of the second-order rate coefficients determined at the different humidities. No dependence of the rate coefficient on water vapour is observed (**b**). Error bars (1σ statistical errors) are partly smaller than the size of the symbols.

In the evaluation of the rate coefficient, systematic errors due to side reactions of the NO reactant need consideration. First, an influence of the photolysis laser on the NO concentration can be excluded because NO does not absorb at 266 nm (Okabe, 1978). However, a small effect is expected from the reaction of NO with ozone forming NO$_2$ in the reaction volume. Under the experimental conditions in this work, a gradual decrease in NO of 1.6 % is expected in the flow tube before the air is sampled by the inlet of the LIF detection cell, using a rate coefficient of the NO reaction with O$_3$ of $k_{NO+O_3} = 1.9 \times 10^{-14}$ cm^3 s^{-1} at a temperature of 298 K (Burkholder et al., 2020). As the rate coefficient for the reaction of OH with NO$_2$ is 1.6 times faster than that with NO, a small bias of +1 % can be estimated for the determination of
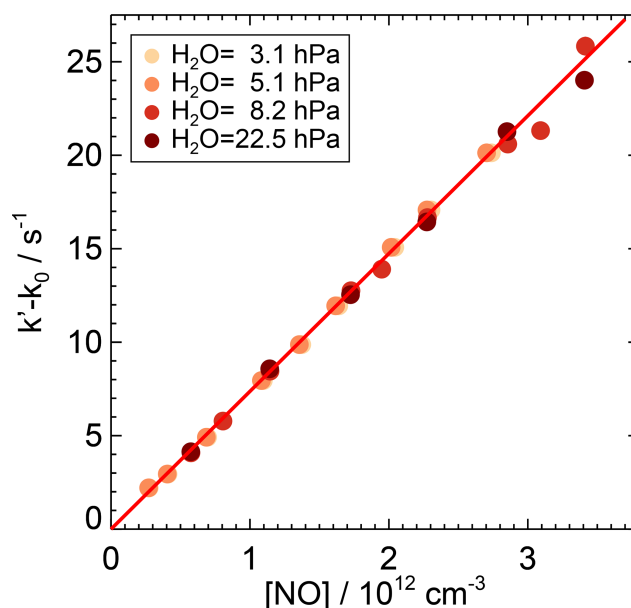
the OH reaction rate with NO due to the formation of NO$_2$. Measured values (Table A1) are corrected for this bias.

The rate coefficient of the OH reaction with NO was derived from the slope of the measured OH reactivity when the NO concentration was varied between 0.2 and 3.5×10^{12} cm^{-3} (Fig. 4, Table A1). The partial water vapour pressure was changed between 3.1 and 22.5 hPa. No significant effect of water vapour on the rate coefficient was observed. The weighted average of the slopes derived from measurements at four different water vapour concentrations gives a rate coefficient of $k_{OH+NO} = (7.3 \pm 0.4) \times 10^{-12}$ cm^3 s^{-1} at a pressure of (1019 ± 3) hPa and a temperature of (297 ± 1) K in air. The total uncertainty is mainly due to the uncertainty in the NO concentrations.

The differences between the rate coefficients in this work and the values recommended by NASA–JPL (Burkholder et al., 2020) and determined by Bohn and Zetzsch (1997) and Bohn and Zetzsch (1999) are less than 4 % (Table 3). Recent work by Sun et al. (2022) provides a parameterisation of the rate coefficient from measurements over a broad pressure range (15 to 990 hPa) at different temperatures (273, 298, 333 K). Their parameterisation gives values which are approximately 13 % lower than those recommended by NASA–JPL for the experimental conditions in this work but agrees better at lower pressures. The measurements in Sun et al.

Table 3. Second-order rate coefficient (k) of the OH reaction with NO in air or N$_2$ at ambient total pressure (p) and temperature (T). In addition, values calculated from the parameterisations in the IUPAC and NASA–JPL recommendations and reported in the literature are given for the conditions in this work. Errors in the rate coefficients are 2σ uncertainties.

k (10^{-12} cm^3 s^{-1})	T (K)	p (hPa)	Bath gas	p(H$_2$O) (hPa)	Reference
4.2 ± 0.8[a]	298	1026	N$_2$	< 4	Overend et al. (1976)
6.7 ± 3.3[b]	296	1013	N$_2$	0.4	Anastasi and Smith (1978)
22 ± 2[a]	295	985	N$_2$	–	Sharkey et al. (1994)
7.4 ± 1.3[c]	297	998	N$_2$	–	Bohn and Zetzsch (1997)
7.1 ± 0.4[d]	297	980	O$_2$	–	Bohn and Zetzsch (1999)
6.3 ± 0.5[a]	298	954	N$_2$	–	Sun et al. (2022)
6.5 ± 0.5[b]	297	1019	N$_2$	–	Sun et al. (2022)
9.9 ± 3.8[e]	297	1019	N$_2$	–	IUPAC (2017b)
7.5 ± 1.5[e]	297	1019	air	–	NASA–JPL, Burkholder et al. (2020)
7.3 ± 0.4[a]	297 ± 1	1019 ± 3	air	3.1–22.5	this work

[a] Measurement for stated conditions. [b] Parameterisation based on measured data. [c] Derived from bi-exponential OH decays in a complex reaction system containing H$_2$O$_2$ and NO. [d] Derived from bi-exponential OH decays in a complex reaction system containing H$_2$O$_2$ and benzene. [e] Parameterisation based on the literature.

(2022) were carried out in N$_2$. The authors assume that the collisional stabilisation of the activated association complex by N$_2$ and O$_2$ is similar so that their parameterisation can also be used for air.

The values recommended by IUPAC (2017b) are 35 % to 50 % higher than the measurements by Sun et al. (2022), Bohn and Zetzsch (1997, 1999), and this work (Fig. 5), suggesting that the IUPAC recommendation may need to be revised.

Sun et al. (2022) also investigated the effect of water vapour on the rate coefficient. Measurements at various water concentrations at low pressure (66 hPa) and room temperature showed a rate coefficient at a water vapour partial pressure of 12 hPa that was 60 % higher than in pure N$_2$. The authors explained this behaviour by the more efficient collisional stabilisation of the activated association complex by water molecules, which was estimated to be a factor of 5 to 6 more efficient than that of N$_2$.

Sun et al. (2022) derived a Troe equation using different low-pressure rate coefficients for N$_2$ and water vapour following the approach described in Amedro et al. (2020). Using the values in Sun et al. (2022), the difference between the rate coefficients for the lowest and highest water vapour concentrations in the experiments in this work is 5 % (Fig. 6). This is higher than the variability in the measured rate coefficients (1 %) determined at the different water vapour concentrations in this work and is a significant discrepancy.

Liessmann et al. (2011) studied the influence of water on the reaction of OH with NO at low total pressures (< 10 hPa) and low temperatures (60 to 300 K). They observed a strong enhancement of the rate coefficient of up to 40 % at a water vapour mixing ratio of 3 % at temperatures below 135 K in a Laval nozzle gas expansion, but the enhancement disappeared at room temperature and became hardly detectable.
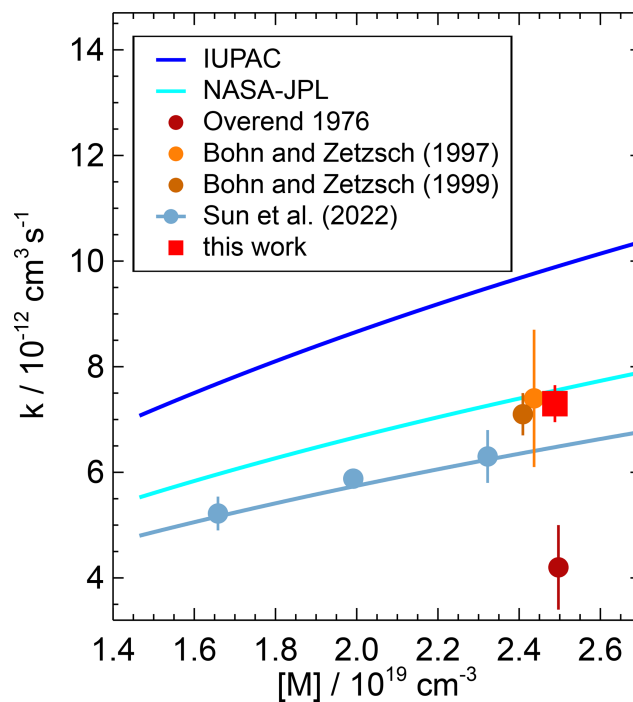

Figure 5. Pressure dependence of the second-order rate coefficient of the OH reaction with NO reported in the literature. Data points represent measured values, and solid lines represent parameterisations using Troe equations. The parameterisation of Sun et al. (2022) (line) is calculated for pure N$_2$ at 297 K, while the corresponding data points were measured at 298 K. Error bars are total errors. The high value measured by Sharkey et al. (1994) (Table 3) is not shown.
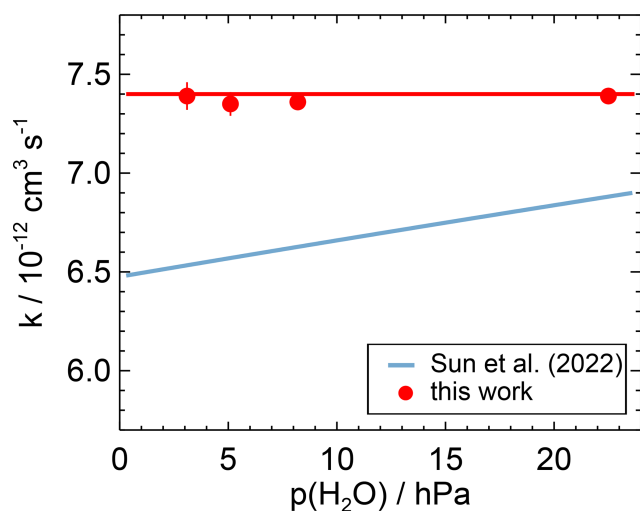
Figure 6. Water vapour dependence of the second-order rate coefficient of the OH reaction with NO measured in this work and calculated from the parameterisation derived in Sun et al. (2022) for the conditions of this work ($T = 297$ K, $p = 1019$ hPa). The horizontal red line is the weighted average of the data measured in this work (Table A1). Error bars (1σ statistical errors) are partly smaller than the size of the symbols.

The results of this work suggest that the efficiency of the collisional stabilisation by water at the conditions in the lower troposphere is smaller than predicted by the parameterisation in Sun et al. (2022). The different behaviour may be due to invalid assumptions in the determination of the parameterisation or due to undetected measurement errors in the data of Sun et al. (2022) or in the present work. More studies are required to resolve this discrepancy.

3.3 Rate coefficient of the OH reaction with NO$_2$

The rate coefficient of the OH reaction with NO$_2$ was measured at a pressure of 1034 hPa, a temperature of 295 K, and two water vapour partial pressures (6.2 and 17.6 hPa, relative humidities 32 % and 90 %) (Table A1). The values were determined from the slope of OH reactivity measurements with varying NO$_2$ concentrations.

The reaction of NO$_2$ with OH can produce either nitric acid (HNO$_3$, Reaction R4) or pernitrous acid (HOONO, Reaction R5). The ratio of the products, HOONO to HNO$_3$, increases with pressure and is (14.2 ± 1.2) % for the experimental conditions of this work (Mollner et al., 2010). Pernitrous acid is thermally unstable and decomposes back to OH and NO$_2$. Its chemical lifetime is approximately 1.2 s at room temperature calculated using the NASA–JPL rate coefficients of the forward reaction and the equilibrium constant (Burkholder et al., 2020). This is a factor of 6 to 36 longer than the OH lifetimes in the experiments in this work. Therefore, the OH decays are expected to represent the sum of the two OH loss reaction channels with little influence of the OH
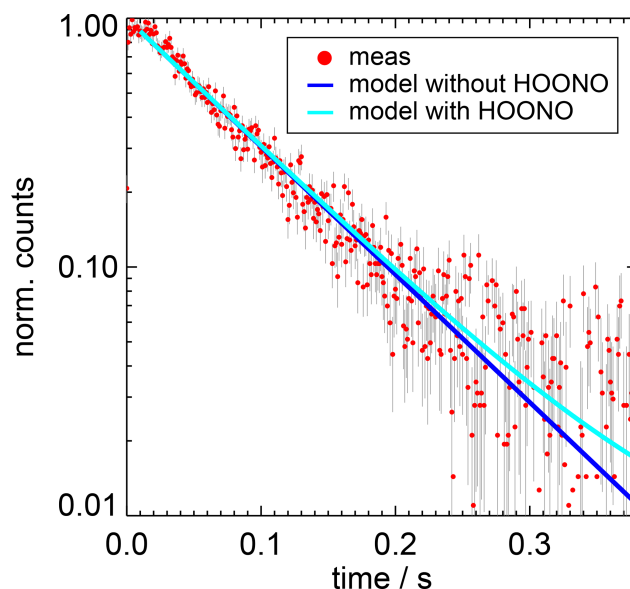

Figure 7. Example of the measured OH decay (normalised counts) and results of simulated decays including either only the OH loss in the reaction with NO$_2$ ("without HOONO") or additionally the OH production from the HOONO decomposition ("with HOONO"). In the example, the corrected OH loss rate is 12.8 s^{-1} and the measurement was performed with an NO$_2$ concentration of 1×10^{12} cm^{-3} and a water vapour partial pressure of 6.2 hPa.

regeneration by the re-dissociation of HOONO. In agreement with the expectation, the observed OH decays showed no obvious deviation from a single exponential behaviour and were first fitted with the expression in Eq. (4).

In order to estimate the small effect of the HOONO decomposition on the derived rate coefficients, the OH decay curves were simulated for two cases using a model that either included or excluded the HOONO decomposition (Fig. 7). The model uses the value of the equilibrium constant (Reaction R5) by NASA–JPL ($K_{eq} = 2.2 \times 10^{12}$ cm^{-3}; Burkholder et al., 2020) and the branching ratio determined by Mollner et al. (2010). The results in Fig. 7 show that the two simulations agree well with the measured OH decay over the 1st order of magnitude and start to diverge from each other only after more than three OH lifetimes, when the noise of the measured decay curve becomes large.

The ratio of the two simulated OH decay curves was used to correct the measured OH decay for the OH production from the HOONO decompositions. Fitting the corrected decay curves to a single exponential function (Eq. 4) gave 3 % to 5 % higher decay rates than without the corrections. The largest effects are obtained for the lowest NO$_2$ concentrations. The corrected OH decay rates (Table A1) were used to calculate the rate coefficients of the OH reaction with NO$_2$ (Fig. 8).

Some other possible systematic errors in the determination of the rate coefficient can be ruled out. (1) The reaction of
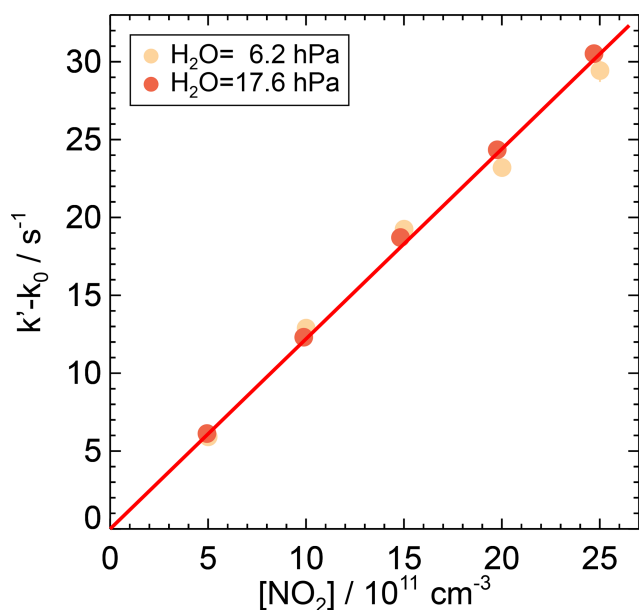
Figure 8. First-order rate coefficients of the OH reaction with NO$_2$ from OH reactivity measurements at ambient temperature (295 K) and pressure (1034 hPa) in air at two partial pressures of water vapour. The zero rate coefficient k_0 is subtracted from the linear fit of the measured OH reactivity (Eq. 7). The slope of the red line is the weighted average of the second-order rate coefficients determined at the different humidities, as there is no observed dependence of the rate coefficient on water vapour. Error bars (1σ statistical errors) are partly smaller than the size of the symbols.

NO$_2$ with O$_3$ is far too slow ($k_{NO_2+O_3} = 3.2 \times 10^{-17}$ cm^3 s^{-1}; Burkholder et al., 2020) to cause a significant change in the NO$_2$ concentration in the flow tube at the given experimental conditions. (2) Although NO$_2$ absorbs at the wavelength of the photolysis laser (266 nm), the effect is negligible since less than 10^{-4} of the NO$_2$ molecules are photodissociated (absorption cross section $\sigma_{NO_2} = 2 \times 10^{-20}$ cm^2; Vandaele et al., 1998) at unity quantum yield. (3) Impurities of NO in the NO$_2$ gas mixture in the gas cylinder showed no detectable impurity of NO (Table 1) and therefore did not affect the determination of the rate coefficient. (4) The formation of NO$_2$ dimers (N$_2$O$_4$) was insignificant as their estimated concentration was about 1.4×10^6 cm^{-3} at the maximum NO$_2$ concentration (2.5×10^{12} cm^{-3}) used in the experiments.

The type of bath gas may also affect the results, as the relative efficiency of the collisional stabilisation of the activated association complex by O$_2$ to N$_2$ is in the range of 0.67 (Mollner et al., 2010) and 0.74 (Amedro et al., 2019). As the experiments in this work were carried out in humidified synthetic air, the measured values refer to rate coefficients in a mixture of 79 % N$_2$ and 21 % O$_2$ and variable traces of water vapour.

The second-order rate coefficients of the OH reaction with NO$_2$ obtained in this work for water vapour partial pressures of 6.2 and 17.2 hPa differed by only 3.3 %, which is slightly

higher than the combined statistical errors (±2.2 %). The weighted average gives a value of $k_{OH+NO_2} = (1.23 \pm 0.04) \times 10^{-11}$ cm^3 s^{-1}. The total error includes the uncertainty of the reactant concentration.

The second-order rate constant in air measured in this work is 4 % higher than the value recommended by IUPAC (2017c) and is 4 % lower than the value recommended by NASA–JPL (Burkholder et al., 2020) (Table 4). The differences between the IUPAC and NASA–JPL recommendations become much larger at low pressure and low temperature as discussed in Amedro et al. (2019). The IUPAC-recommended values are given for N$_2$ as a bath gas, whereas the NASA–JPL recommendation takes into account the differences in the collisional stabilisation of the activated association complex by N$_2$ and O$_2$. If this effect was taken into account in the IUPAC recommendation, the rate coefficient would be approximately 3 % lower (Amedro et al., 2019), further increasing the difference between the values of the IUPAC and NASA–JPL recommendations. This also affects the agreement with the value determined in this work. However, the resulting difference is still smaller than the uncertainty of the recommendations (Table 4).

Few other studies have measured the rate coefficient at ambient pressure, which is in the fall-off region (Fig. 9). The rate coefficients in two recent studies (Amedro et al., 2019; Winiberg et al., 2020) that derived Troe expressions (Eq. 1) agree well to within ±2 % (Table 4). The value obtained in the study by Mollner et al. (2010) is approximately 15 % lower than the values obtained in the more recent studies. Possible reasons for the lower value in Mollner et al. (2010) are discussed in Amedro et al. (2019), including possible systematic errors in the determination of the NO$_2$ concentration, but the exact reason remains unclear.

Amedro et al. (2020) determined the effect of collisional stabilisation of the association complex by water molecules in experiments at low pressure and high partial pressures of water vapour. These experiments show that the collision efficiency is 6 times higher than for N$_2$, similar to the effect on the OH reaction with NO (Sun et al., 2022). Using the Troe equation determined by Amedro et al. (2020) for N$_2$–H$_2$O mixtures, the rate coefficient increases by 2.7 % for water vapour partial pressures of 6.2 and 17.2 hPa tested in this work (Fig. 10). The prediction is in good agreement with the increase in the rate coefficients of (3.3 ± 2.2) % observed in this work (Fig. 10).

Sadanaga et al. (2006) found that the reaction rate coefficient decreases by 18 % when the partial pressure of water vapour is increased from 4 to 29 hPa. The experimental conditions were similar to those in this work in terms of bath gas, temperature, and pressure, and similar OH reactivity instruments were used. It is worth noting that the rate coefficients determined in the work by Sadanaga et al. (2006) for water vapour partial pressures higher than 10 hPa are in good agreement with the rate coefficients in this work (Fig. 10). However, the increase in the rate coefficient at

Table 4. Second-order rate coefficient (k) of the OH reaction with NO$_2$ in air or N$_2$ at ambient total pressure (p) and temperature (T). In addition, values calculated from the parameterisation in the IUPAC and NASA–JPL recommendations and reported in the literature are given for the conditions in this work. Errors in the rate coefficients are 2σ uncertainties.

k (10^{-11} cm^3 s^{-1})	T (K)	p (hPa)	Bath gas	p(H$_2$O) (hPa)	Reference
1.40 ± 0.1^a	298	990	air	3.7	Sadanaga et al. (2006)
1.06 ± 0.1^b	298	1013	air	–	Mollner et al. (2010)
1.21 ± 0.1^b	298	1013	air	–	Amedro et al. (2019)
1.25 ± 0.2^a	293	1000	N$_2$/air	–	Winiberg et al. (2020)
1.08 ± 0.1^b	295	1034	air	–	Mollner et al. (2010)
1.26 ± 0.1^b	295	1034	air	–	Amedro et al. (2019)
1.22 ± 0.15^b	295	1034	N$_2$/air	–	Winiberg et al. (2020), JPL expression
1.18 ± 0.55^c	295	1034	N$_2$	–	IUPAC (2017c)
1.28 ± 0.34^c	295	1034	air	–	NASA–JPL (Burkholder et al., 2020)
$1.23 \pm 0.04^{a,d}$	295	1034	air	6.2, 17.6	this work

^{a} Measurement for stated conditions. ^{b} Parameterisation based on measured data. ^{c} Parameterisation based on the literature. ^{d} Decay curves corrected for HOONO decomposition.

lower water vapour pressure contradicts the results in the present work and in Amedro et al. (2020). Theoretical calculations in Sadanaga et al. (2006) could not explain their observed water vapour dependence. Therefore, the discrepancies with the recent studies remain unexplained.

3.4 Rate coefficient of the HO$_2$ reaction with NO$_2$

The reaction of HO$_2$ with NO$_2$ was studied in this work in air at a total pressure of 1031 hPa at a temperature of 297 K for different water vapour partial pressures between 2.0 hPa and 17.5 hPa equivalent to relative humidities between 11 % and 90 %. For these measurements, the instrument was operated to produce HO$_2$ in the flow and to detect the HO$_2$ decay (Sect. 2.1). The HO$_2$ reaction with NO$_2$ forms pernitric acid (HO$_2$NO$_2$) in a termolecular reaction (Reaction R8).

Several potential systematic errors in the determination of the rate coefficients can be excluded:

- HO$_2$NO$_2$ is thermally unstable (Gierczak et al., 2005) and could affect the HO$_2$ decay by producing HO$_2$. The chemical lifetime of HO$_2$NO$_2$ was approximately 10 s calculated using the NASA–JPL equilibrium constant and reaction rates (Burkholder et al., 2020). This is much longer than the timescale of the experiments in this work. Consequently, no deviations from single-exponent behaviour were observed.

- As discussed for the OH reaction with NO$_2$ (Sect. 3.3), laser photolysis of NO$_2$ was negligible, since less than 10^{-4} of the NO$_2$ molecules were photolysed, and thus the NO$_2$ concentration did not change. Although NO produced in the photolysis of NO$_2$ can react with HO$_2$, this does not affect the observed HO$_2$ decay because the OH produced reacts back to HO$_2$ in the reaction with excess CO.

- The reaction of HO$_2$ with NO from impurities in the NO$_2$ mixture of the air supply (Table 1) or from NO$_2$ photolysis could have contributed to the total HO$_2$ loss. However, the expected NO concentrations were very low and the NO reaction with HO$_2$ produces OH, which immediately reacted back to HO$_2$ in the reaction with excess CO (Sect. 2.1).

- Systematic errors due to the self-reaction of HO$_2$, as reported in previous studies (e.g. Kurylo and Ouellette, 1986; Christensen et al., 2004), were negligible due to the very low initial HO$_2$ concentrations used in this work (Sect. 2.3).

Measurements were performed at different water vapour partial pressures. The rate coefficients increased linearly by approximately 20 % as the water vapour partial pressure increased from 2.0 to 17.5 hPa (Fig. 11, Table A1). The observed linear dependence on water concentration can be empirically described by

$$k_{\text{HO}_2+\text{NO}_2}^{\text{eff}} = k_{\text{HO}_2+\text{NO}_2} + k_{\text{HO}_2+\text{NO}_2}^{\text{H}_2\text{O}} [\text{H}_2\text{O}], \tag{8}$$

where $k_{\text{HO}_2+\text{NO}_2}^{\text{eff}}$ is the measured second-order rate coefficient determined from the observed HO$_2$ decays. The rate coefficient $k_{\text{HO}_2+\text{NO}_2}$ represents the value in dry air at 1 atm, and $k_{\text{HO}_2+\text{NO}_2}^{\text{H}_2\text{O}}$ is a third-order rate coefficient that describes the enhancement of the observed rate coefficient by water vapour. A linear fit of the measurements (Fig. 11) yields values of $k_{\text{HO}_2+\text{NO}_2} = (1.56 \pm 0.05) \times 10^{-12}$ cm^3 s^{-1} and $k_{\text{HO}_2+\text{NO}_2}^{\text{H}_2\text{O}} = (0.92 \pm 0.09) \times 10^{-30}$ cm^6 s^{-1}. The errors are total uncertainties that include the measurement errors and the uncertainties in the NO$_2$ and H$_2$O concentrations.

Sander and Peterson (1984) observed a similar behaviour and proposed an enhanced rate coefficient of the NO$_2$ reaction with the hydrogen-bonded HO$_2 \cdot$ H$_2$O complex.

$$\text{HO}_2 \cdot \text{H}_2\text{O} + \text{NO}_2 \rightarrow \text{HO}_2\text{NO}_2 + \text{H}_2\text{O} \tag{R11}$$
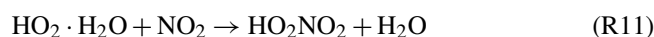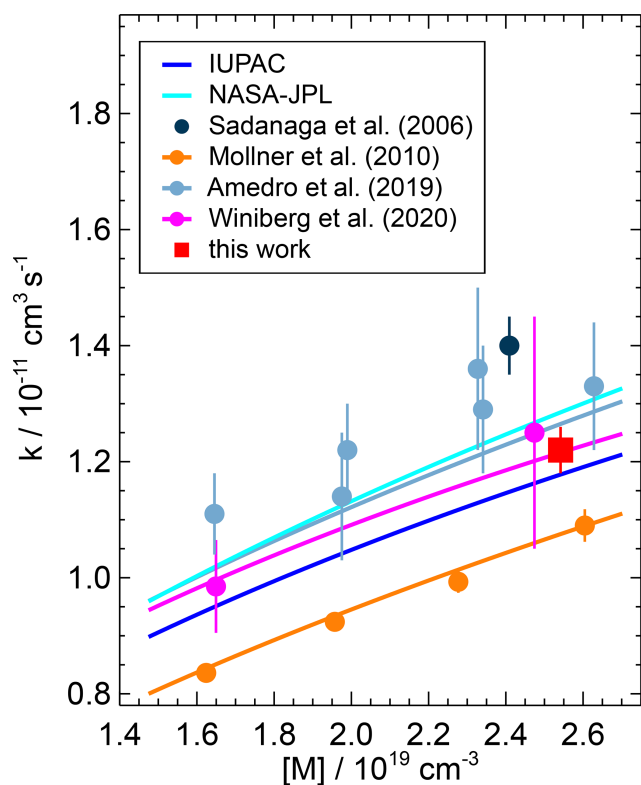
Figure 9. Pressure dependence of the second-order rate coefficient for the OH reaction with NO_2 reported in the literature. Data points represent measured values, and solid lines represent parameterisations using Troe equations. The parameterisation of Winiberg et al. (2020) is the NASA–JPL-type Troe equation given in their work. The parameterisations are calculated for the temperature used in the present study (295 K), but the measured data points shown were obtained at slightly different conditions (Mollner et al. (2010): $T = 298$ K; Amedro et al. (2019): $T = 298$ K, N_2 bath gas; Winiberg et al. (2020): $T = 293$ K). Error bars are total errors.

The bimolecular rate coefficient of this reaction can be determined from the observed water vapour dependence, taking into account the chemical equilibrium between the free HO_2 radical and the $HO_2 \cdot H_2O$ complexes, which are in a fast equilibrium (e.g. Cox and Burrows, 1979; Aloisio et al., 2000).

$$HO_2 + H_2O \rightleftharpoons HO_2 \cdot H_2O \qquad (R12)$$

Kanno et al. (2005) determined the value of the equilibrium constant at room temperature to be $K_{eq} = (5.2 \pm 3.2) \times 10^{-19}$ cm³, which is in good agreement with the results of other studies (Cox and Burrows, 1979; Lii et al., 1981; Aloisio et al., 2000) and is also the value recommended by NASA–JPL (Burkholder et al., 2020), where the uncertainty is estimated to be a factor of 2. The equilibrium can be assumed to be instantaneous on the timescale of the HO_2 decay in the flow tube of the instrument used in this work. The fraction f of the free HO_2 radicals can be estimated by the
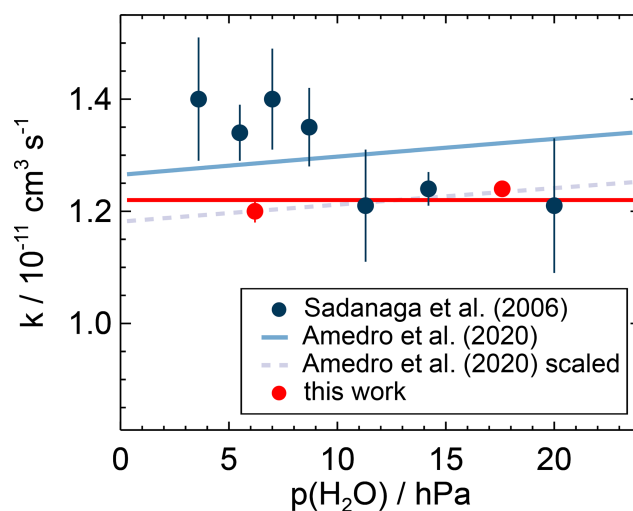

Figure 10. Water vapour dependence of the second-order rate coefficient of the OH reaction with NO_2 measured in this work and calculated from the parameterisation of the measurements in Amedro et al. (2020) for conditions of this work (air, $T = 295$ K, $p = 1034$ hPa). The parameterisation fits the measured data of this work when scaled by a factor of 0.93. The measurements of Sadanaga et al. (2006) were made at a temperature of 298 K and a pressure of 990 hPa in air.

following approach:

$$f = \frac{[HO_2]}{[HO_2] + [HO_2 \cdot H_2O]} = \frac{[HO_2]}{[HO_2] + K_{eq}[H_2O][HO_2]}$$
$$= \frac{1}{1 + K_{eq}[H_2O]} \approx 1 - K_{eq}[H_2O], \qquad (9)$$

where $K_{eq}[H_2O]$ is a small number (< 0.2) for the range of water vapour concentrations used in this work and represents the concentration ratio of the complexed HO_2 to free HO_2 radicals (Fig. 11).

The detection of HO_2 in the low-pressure detection cell of the instrument can be assumed to be equally sensitive to the free HO_2 radical and the HO_2–water complex. Calibration measurements show that the HO_2 detection sensitivity decreases slightly by 15 % with increasing water vapour concentrations in the range used in this work. This can be quantitatively explained by fluorescence quenching by water molecules (Fuchs et al., 2011), providing evidence for the same instrument sensitivity for the free HO_2 radical and the HO_2–water complex.
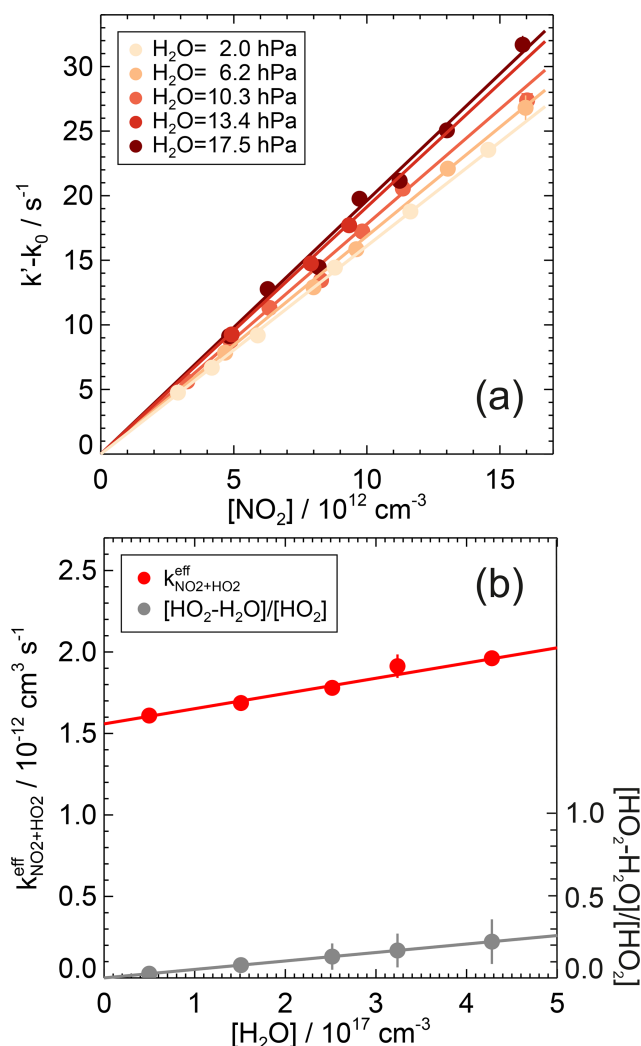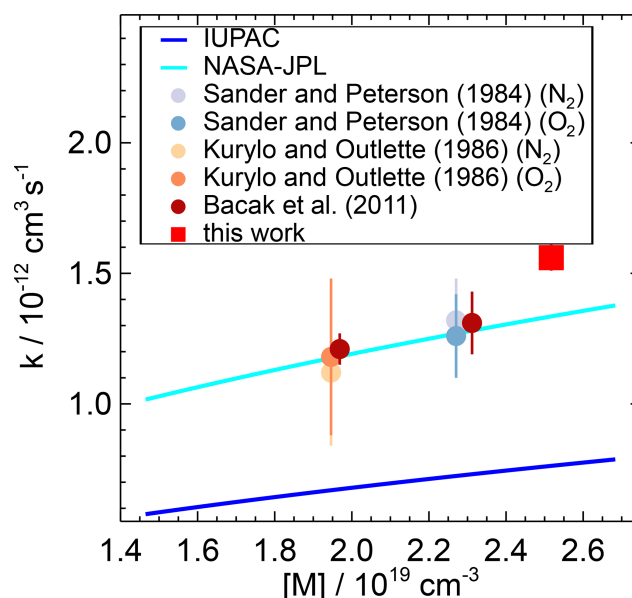
Figure 12. Pressure dependence of the second-order rate coefficient of the HO_2 reaction with NO_2 reported in the literature and measured in this work. IUPAC and NASA–JPL values are calculated for the conditions of this work ($T = 297$ K), and measurements of Bacak et al. (2011) were performed in N_2 at room temperature (298 K) and a pressure of 933 hPa. Error bars are total errors.

This approach gives a linear dependence of the effective rate coefficient, $k_{HO_2+NO_2}^{eff}$, on water vapour, as observed (Fig. 11).

$$k_{HO_2+NO_2}^{eff} = k_{HO_2+NO_2} + (k_{HO_2\cdot H_2O+NO_2} - k_{HO_2+NO_2}) \cdot K_{eq}[H_2O] \tag{11}$$

Comparing the empirical expression of the H_2O dependence (Eq. 8) with Eq. (11) and using the observed values (Table 5) allow us to calculate the value of the second-order rate coefficient for the NO_2 reaction with the HO_2–water complex (Reaction R11). This yields a value of $k_{HO_2\cdot H_2O+NO_2} = (3.4 \pm 1.1) \times 10^{-12}$ cm^3 s^{-1}. The uncertainty is higher than for the other rate coefficients due to the uncertainty of the equilibrium constant (Kanno et al., 2005).

The enhancement of the rate coefficient for the HO_2–water complex can be explained by the Chaperone mechanism, where the water molecule bonded to HO_2 acts as a third body that removes energy and stabilises the association product of the reaction between HO_2 and NO_2 similar to the mechanism discussed in Christensen et al. (2004) for the methanol-bonded HO_2 radical.

To the best of our knowledge, our study provides the first experimental data on the HO_2 reaction with NO_2 in 1 atm air. Previous studies were mostly carried out at lower total pressures, and only the study by Bacak et al. (2011) was carried

Figure 11. First-order rate coefficients for the reaction of HO_2 with NO_2 at different humidities and ambient temperature ((297 ± 1) K) and pressure ((1026 ± 5) hPa) in air (**a**). The zero rate coefficient k_0 is subtracted from the linear fit of the measured HO_2 reactivity (Eq. 7). The lines are the results of a linear fit to the measurements at each humidity. The rate coefficients show a linear increase with the water vapour concentration, which scales with the concentration ratio of HO_2 complexed with H_2O to free HO_2 radicals (**b**). Error bars (1σ statistical errors) are partly smaller than the size of the symbols.

The observed radical decay using Eq. (9) is then given by

$$\frac{d([HO_2] + [HO_2 \cdot H_2O])}{dt} = \left(f \cdot k_{HO_2+NO_2}\right.$$
$$+ (1-f) \cdot k_{HO_2\cdot H_2O+NO_2}\big) [NO_2]([HO_2]$$
$$+ [HO_2 \cdot H_2O])$$
$$\approx \left(k_{HO_2+NO_2} + (k_{HO_2\cdot H_2O+NO_2} - k_{HO_2+NO_2})\right.$$
$$\cdot K_{eq}[H_2O]\big) \cdot [NO_2]([HO_2] + [HO_2 \cdot H_2O])$$
$$= k_{HO_2+NO_2}^{eff}[NO_2]([HO_2] + [HO_2 \cdot H_2O]). \tag{10}$$

Table 5. Second-order rate coefficients for the reaction of the free HO$_2$ radical and the HO$_2$–water complex with NO$_2$ and the third-order rate coefficient describing the water dependence at ambient pressure (p) and temperature (T), as well as varying humidity, determined in this work. In addition to the IUPAC and NASA–JPL recommendations (values calculated for the experimental conditions), the results of experiments reported in the literature are given. The errors in the rate coefficients are 2σ uncertainties.

Reaction	Rate coefficient	T (K)	p (hPa)	Bath gas	p(H$_2$O) (hPa)	Reference
HO$_2$ + NO$_2$	$(1.31 \pm 0.12) \times 10^{-12}$ cm^3 s^{-1} [a]	298	950	N$_2$	–	Bacak et al. (2011)
	$(0.76 \pm 0.19) \times 10^{-12}$ cm^3 s^{-1} [b]	297	1031	N$_2$	–	IUPAC (2017a)
	$(1.34 \pm 0.08) \times 10^{-12}$ cm^3 s^{-1} [b]	297	1031	air	–	NASA–JPL (Burkholder et al., 2020)
	$(1.56 \pm 0.05) \times 10^{-12}$ cm^3 s^{-1} [c]	297	1031	air	0	this work
HO$_2 \cdot$ H$_2$O + NO$_2$	2.9×10^{-12} cm^3 s^{-1} [d,e]	298	467	N$_2$	0–21	Sander and Peterson (1984)
	$(3.4 \pm 1.1) \times 10^{-12}$ cm^3 s^{-1} [d]	297	1031	air	2.0–17.5	this work
HO$_2$ + NO$_2$ + H$_2$O	1.0×10^{-30} cm^6 s^{-1} [f]	298	467	N$_2$	0–21	Sander and Peterson (1984)
	$(0.92 \pm 0.09) \times 10^{-30}$ cm^6 s^{-1} [f]	297	1031	air	2.0–17.5	this work

[a] Measurement for stated conditions. [b] Parameterisation based on the literature. [c] Calculated from the fit results Eq. 8 (Fig. 11). [d] Calculated from the fit results Eq. (8) (Fig. 11) using $K_{eq} = 5.2 \times 10^{-19}$ cm^3 (Kanno et al., 2005). [e] Re-calculated. [f] Termolecular reaction rate constant Eq. 8.

out under conditions close to those of this work (950 hPa in N$_2$ in a turbulent flow tube; Table 4, Fig. 12).

The rate coefficient derived in this work for the NO$_2$ reaction with the free HO$_2$ radical is a factor of 2 higher than the IUPAC (2017a) recommendation and 17 % higher than the NASA–JPL recommendation (Burkholder et al., 2020) (Table 5, Fig. 12). The NASA–JPL recommendation for room temperature is based on measurements by Sander and Peterson (1984), Kurylo and Ouellette (1986), Christensen et al. (2004), and Bacak et al. (2011). In these studies, the rate coefficients were measured at lower-than-ambient pressures between 250 and 950 hPa and temperatures between 277 and 298 K. A recent re-analysis of the rate coefficients available in the literature using a master equation analysis by McKee et al. (2022) gave a parameterisation which agrees well with the values recommended by NASA–JPL.

The IUPAC recommendation is based only on measurements by Christensen et al. (2004), where experiments were performed at much lower-than-ambient pressures ($<$ 270 hPa). IUPAC excludes the studies by Sander and Peterson (1984) and Kurylo and Ouellette (1986) from their analysis because in these studies HO$_2$ was produced using methanol as a precursor. This can affect the results by the formation of a hydrogen-bonded adduct with HO$_2$, as the adduct can introduce a systematic error at temperatures below 250 K due to an increased rate of the NO$_2$ reaction with the methanol–HO$_2$ complex (Christensen et al., 2004). The large discrepancy between the NASA–JPL and IUPAC predictions in the fall-off region around 1 atm may therefore be caused by the different data sets parameterised over different pressure ranges and/or by the use of different broadening factors in the Troe equations. Both recommendations underestimate the value determined in this work, indicating the need for more extensive experimental studies covering a wider pressure range around 1 atm.

The effect of an increasing effective reaction rate in the presence of water was also observed in the experiments of

Sander and Peterson (1984), which were carried out at room temperature and a low pressure of 467 hPa with water vapour partial pressures between 0 and 21 hPa in N$_2$. They determined a third-order rate coefficient $k_{HO_2+NO_2}^{H_2O}$ (Eq. 8) of 1.0×10^{-30} cm^6 s^{-1} which is very close to the value of this work in 1 atm air (Table 5). It should be noted, however, that the expression for the rate coefficient $k_{HO_2+NO_2}^{H_2O}$ includes the pressure-dependent second-order rate coefficient $k_{HO_2+NO_2}$, so the agreement is not necessarily expected. However, the pressure sensitivity is small at room temperature because the value is mainly determined by the pressure-independent rate coefficient $k_{HO_2 \cdot NO_2+NO_2}$, which is a factor 2 to 3.5 higher than the pressure-dependent rate coefficient $k_{HO_2+NO_2}$ for the conditions of the two studies.

Sander and Peterson (1984) also derived a relationship similar to that in Eq. (10) to determine the second-order rate coefficient for the NO$_2$ reaction with the HO$_2$–water complex but did not substitute [HO$_2$] with [HO$_2$] + [HO$_2 \cdot$ H$_2$O]/(1 + K_{eq}) in their rate equation. Using Eq. (11) and the latest recommendation for K_{eq} (Kanno et al., 2005; Burkholder et al., 2020), the re-calculation of the second-order rate coefficient gives a value of 2.9×10^{-12} m^3 s^{-1} for their data. The difference with the value in this work is 14 %, but this is well within the measurement errors in both studies. The similarity of the values obtained in Sander and Peterson (1984) and in this work at different total pressures (467 and 1031 hPa) supports the assumption that the reaction follows a Chaperone mechanism that is independent of the buffer gas (N$_2$, air).

An increase in the HO$_2$ reactivity due to the complexation with water molecules has been observed for other reactions, such as the self-reaction of HO$_2$, which can be enhanced by a factor of up to 2 in the moist troposphere (Lii et al., 1981; Kircher and Sander, 1984). Christensen et al. (2004) reported a similar effect for methanol, which also forms an adduct with HO$_2$ and increases the reaction rate between HO$_2$ and NO$_2$.

A temperature dependence of the rate coefficient of the NO_2 reaction with the HO_2–water complex can be estimated from measured data in Sander and Peterson (1984), which supports the assumption that the reaction of complexed HO_2 with NO_2 follows a bimolecular mechanism. In their work, they measured an increase in the value by a factor of 1.3 and 1.6 when the temperature was reduced from 298 to 286 K and 275 K, respectively. A re-calculation of their values (see above) gives a temperature trend with a positive Arrhenius activation energy $E/R = 1220$ K. In contrast, the pressure-dependent NO_2 reaction with the free HO_2 radical shows a negative temperature dependence. The water dependence of the HO_2 reaction with NO_2 is therefore expected to increase in warmer regions. For example, increasing the temperature by 10 degrees at 298 K and 1 atm increases the ratio of the rate coefficients $k_{HO_2 \cdot H_2O + NO_2} : k_{HO_2 + NO_2}$ from 2.1 to 2.6.

Higher temperatures also mean higher concentrations of water vapour in the atmosphere. However, this does not necessarily increase the concentration of the $HO_2 \cdot H_2O$ complex because the equilibrium (Reaction R12) is shifted towards free HO_2 radicals at higher temperatures. Overall, the influence of water vapour on the reaction of HO_2 with NO_2 is complex and remains uncertain mainly because the equilibrium constant has a large uncertainty and because of the general lack of reaction kinetic measurements with water vapour over the tropospheric temperature range.

4 Conclusions

The second-order rate coefficients of the termolecular reactions of OH with CO, NO, and NO_2 and of the termolecular reaction of HO_2 with NO_2 were measured at tropospheric conditions of 1 atm pressure, at room temperature, and using humidified air as bath gas. The water vapour partial pressure was varied between 2.0 and 22.5 hPa. An instrument, which was developed for the measurement of atmospheric OH reactivity in field and chamber experiments (Lou et al., 2010), was used. This instrument measures the decay of OH radicals produced by laser flash photolysis of ozone using laser-induced fluorescence with a high sensitivity. The accuracies of the rate coefficients obtained in this work are better than 5 %, mainly limited by the uncertainty of the certified commercial reactant gas standards, whose concentrations were checked using independent reference instruments.

Except for the rate coefficient of the HO_2 reaction with NO_2, the measured values are within the range of the recommendations of IUPAC and NASA–JPL evaluations, which partly specify large uncertainties. The experimental method used in this work yields rate coefficients which are among the most accurate values reported so far for atmospheric conditions. It is worth noting that the kinetic decays were carried out on a timescale similar to that of OH reactions in the lower troposphere. The initial OH concentrations were a factor of 10 to 10 000 lower than in all previous studies, and the corre-

sponding reactant concentrations were about a factor of 1000 lower, greatly reducing the potential for perturbation by secondary chemistry.

Measurements of the rate coefficient for the OH reaction with CO are in very good agreement with the NASA–JPL and IUPAC values. The differences are less than the 5 % uncertainty of the value determined in this work. The rate coefficient of the OH reaction with NO agrees within 3 % with the NASA–JPL value, whereas the IUPAC value is 35 % higher than in this work and 50 % higher than the recently measured value by Sun et al. (2022). This suggests that the IUPAC recommendation may need to be revised. The rate coefficient for the reaction of the OH reaction with NO_2 measured in this work in air is 4 % lower than the NASA–JPL-recommended value in air and is 4 % higher than the IUPAC-recommended value. Since the collisional stabilisation of the activated association complex is different for N_2 and O_2 (Amedro et al., 2019), the IUPAC value which is given for N_2 would be additionally 3 % lower in air.

Due to the large abundance of water vapour in the troposphere, it is an important question to what extent H_2O influences atmospheric reactions by acting as a third-body collision partner or by forming a complex with OH or HO_2. In agreement with the literature, no significant influence of H_2O was found for the reaction of OH with CO for water vapour partial pressures up to 22.5 hPa on water in 1 atm air at room temperature.

The activated association complexes formed in the OH reactions with NO and NO_2 have been shown to be better stabilised by water molecules than by N_2 and O_2 (Paraskevopoulos and Irwin, 1984; Amedro et al., 2020; Sun et al., 2022). However, the effect becomes small at pressures of 1 atm and water concentrations typically found in the lower troposphere and tested in this work.

For the reaction of OH with NO, recent work by Sun et al. (2022) predicts an increase in the rate constant of up to 5 % for the range of water concentrations in this work. However, the observed variability in this work is only 1 %, suggesting that the effect is smaller than expected from the results in Sun et al. (2022). The rate coefficients of the reaction of OH with NO_2 were measured for two water vapour partial pressures (6 and 17 hPa). The small increase in the values of (3.3 ± 2.2) % with increasing water vapour agrees with a prediction of 2.7 % from the Troe equation determined by Amedro et al. (2020). A negative dependence on water vapour reported for atmospheric conditions in air by Sadanaga et al. (2006) could not be confirmed.

A strong water vapour dependence of the effective reaction rate coefficient was found for the reaction of HO_2 with NO_2 giving a second-order rate coefficient for dry air at 1 atm pressure that is a factor of 2 larger than the recommendation by IUPAC for N_2 and 17 % higher than the NASA–JPL-recommended value for air. The measured rate coefficient shows a linear increase of 25 % at a water vapour partial pressure of 17.5 hPa. Similar to the well-known water-

dependent HO_2 self-reaction, the increased reactivity is presumably caused by HO_2 radicals that form a complex with water molecules which reacts faster with NO_2 than free HO_2 radicals.

The observed increase can be explained by the known thermal equilibrium between free HO_2 radicals and HO_2 radicals complexed with H_2O (Cox and Burrows, 1979; Aloisio et al., 2000). This can be used to determine the second-order rate coefficient for the reaction of the $HO_2 \cdot H_2O$ complex with NO_2 resulting in a value that is a factor of 2 faster than that of the reaction of the free HO_2 radical.

A re-analysis of the data of Sander and Peterson (1984), who studied the water vapour dependence of this reaction at a pressure of 467 hPa and room temperature, gives a good agreement of the rate coefficients of the $HO_2 \cdot H_2O$ complex with NO_2 with the value determined in this work at 1031 hPa. This agreement supports the assumption that the reaction of the $HO_2 \cdot H_2O$ complex with NO_2 behaves like a pressure-independent bimolecular reaction. Although the rate coefficient of this Chaperone-type reaction has a large uncertainty, the results suggest that the water effect should be included in atmospheric chemistry models. It also demonstrates the general need to consider potential water effects of reactions relevant in the atmosphere, as discussed in the review by Buszek et al. (2011) and shown in global chemical transport models (Khan et al., 2015).

Overall, the measurements in this work provide highly accurate rate coefficients that can serve as reference values at tropospheric conditions and could be used to improve the parameterisation of termolecular rate coefficients (Burkholder et al., 2017; Fiore et al., 2024). The method of using an OH reactivity instrument for kinetic studies can be extended to also measure the temperature dependence of the rate coefficient, as successfully shown by Berg et al. (2024) for the OH reactions with alkanes, aromatics, and monoterpenes.

Appendix A: Measured rate coefficients

Table A1. Second-order rate coefficients (k) determined in this study. Errors are 1σ statistical errors and do not include the uncertainty of the reactant's concentration.

Reaction	k (cm^3 s^{-1})	T (K)	p (hPa)	$p(\text{H}_2\text{O})$ (hPa)
OH + CO	$(2.32 \pm 0.05) \times 10^{-13}$	295	1009	3.0
	$(2.42 \pm 0.03) \times 10^{-13}$	295	1009	5.1
	$(2.35 \pm 0.01) \times 10^{-13}$	298	1022	8.2
	$(2.42 \pm 0.01) \times 10^{-13}$	299	1025	20.5
OH + NO	$(7.39 \pm 0.07) \times 10^{-12a}$	296	1016	3.1
	$(7.28 \pm 0.06) \times 10^{-12a}$	296	1018	5.1
	$(7.29 \pm 0.03) \times 10^{-12b}$	298	1023	8.2
	$(7.32 \pm 0.03) \times 10^{-12b}$	298	1022	22.5
OH + NO$_2$	$(1.20 \pm 0.02) \times 10^{-11c}$	295	1034	6.2
	$(1.24 \pm 0.01) \times 10^{-11c}$	295	1034	17.6
HO$_2$ + NO$_2$	$(1.61 \pm 0.02) \times 10^{-12}$	297	1021	2.0
	$(1.69 \pm 0.05) \times 10^{-12}$	297	1031	6.2
	$(1.78 \pm 0.02) \times 10^{-12}$	297	1031	10.3
	$(1.73 \pm 0.04) \times 10^{-12}$	297	1032	13.4
	$(1.96 \pm 0.02) \times 10^{-12}$	297	1031	17.5

[a] Using the NO gas mixture from cylinder B (Table 1). [b] Using the NO gas mixture from cylinder B (Table 1). [c] Decay curves corrected for HOONO decomposition.

References

Aloisio, S. and Francisco, J. S.: A density functional study of the H$_2$O$-$-HOCO complex, J. Phys. Chem. A, 104, 404–407, https://doi.org/10.1021/jp9928356, 2000.

Aloisio, S., Francisco, J. S., and Friedl, R. R.: Experimental evidence for the existence of the HO$_2$–H$_2$O complex, J. Phys. Chem. A, 104, 6597–6601, https://doi.org/10.1021/jp0006330, 2000.

Amedro, D., Miyazaki, K., Parker, A., Schoemaecker, C., and Fittschen, C.: Atmospheric and kinetic studies of OH and HO$_2$ by the FAGE technique, J. Environ. Sci., 24, 78–86, https://doi.org/10.1016/S1001-0742(11)60723-7, 2012.

Amedro, D., Bunkan, A. J. C., Berasategui, M., and Crowley, J. N.: Kinetics of the OH + NO$_2$ reaction: rate coefficients (217–333 K, 16–1200 mbar) and fall-off parameters for N$_2$ and O$_2$ bath gases, Atmos. Chem. Phys., 19, 10643–10657, https://doi.org/10.5194/acp-19-10643-2019, 2019.

Amedro, D., Berasategui, M., Bunkan, A. J. C., Pozzer, A., Lelieveld, J., and Crowley, J. N.: Kinetics of the OH + NO$_2$

reaction: effect of water vapour and new parameterization for global modelling, Atmos. Chem. Phys., 20, 3091–3105, https://doi.org/10.5194/acp-20-3091-2020, 2020.

Anastasi, C. and Smith, I. W. M.: Rate measurements of reactions of OH by resonance absorption. Part 6. Rate constants for OH + NO(+M) → HNO$_2$(+M) over a wide range of temperature and pressure, J. Chem. Soc. Farad. Trans., 74, 1056–1064, https://doi.org/10.1039/F29787401056, 1978.

Atkinson, R., Baulch, D. L., Cox, R. A., Crowley, J. N., Hampson, R. F., Hynes, R. G., Jenkin, M. E., Rossi, M. J., and Troe, J.: Evaluated kinetic and photochemical data for atmospheric chemistry: Volume I – gas phase reactions of O$_x$, HO$_x$, NO$_x$ and SO$_x$ species, Atmos. Chem. Phys., 4, 1461–1738, https://doi.org/10.5194/acp-4-1461-2004, 2004.

Atkinson, R., Baulch, D. L., Cox, R. A., Crowley, J. N., Hampson, R. F., Hynes, R. G., Jenkin, M. E., Rossi, M. J., Troe, J., and IUPAC Subcommittee: Evaluated kinetic and photochemical data for atmospheric chemistry: Volume II – gas phase reactions of organic species, Atmos. Chem. Phys., 6, 3625–4055, https://doi.org/10.5194/acp-6-3625-2006, 2006.

Bacak, A., Cooke, M. C., Bardwell, M. W., McGillen, M. R., Archibald, A. T., Huey, L. G., Tanner, D., Utembe, S. R., Jenkin, M. E., Derwent, R. G., Shallcross, D. E., and Percival, C. J.: Kinetics of the HO$_2$ + NO$_2$ reaction: On the impact of new gas-phase kinetic data for the formation of HO$_2$NO$_2$ on HO$_X$, NO$_X$ and HO$_2$NO$_2$ levels in the troposphere, Atmos. Environ., 45, 6414–6422, https://doi.org/10.1016/j.atmosenv.2011.08.008, 2011.

Barker, J. R., Stanton, J. F., and Nguyen, T. L.: Semiclassical transition state theory/master equation kinetics of HO + CO: Performance evaluation, Int. J. Chem. Kin., 52, 1022–1045, https://doi.org/10.1002/kin.21420, 2020.

Beno, M. F., Jonah, C. D., and Mulac, W. A.: Rate constants for the reaction OH + CO as functions of temperature and water concentration, Int. J. Chem. Kin., 17, 1091–1101, https://doi.org/10.1002/kin.550171006, 1985.

Berg, F., Novelli, A., Dubus, R., Hofzumahaus, A., Holland, F., Wahner, A., and Fuchs, H.: Temperature-dependent rate coefficients for the reactions of OH radicals with selected alkanes, aromatic compounds, and monoterpenes, Atmos. Chem. Phys., 24, 13715–13731, https://doi.org/10.5194/acp-24-13715-2024, 2024.

Bohn, B. and Zetzsch, C.: Rate Constants of HO$_2$ + NO Covering Atmospheric Conditions. 1. HO$_2$ Formed by OH + H$_2$O$_2$, J. Phys. Chem. A, 101, 1488–1493, https://doi.org/10.1021/jp961396x, 1997.

Bohn, B. and Zetzsch, C.: Gas-phase reaction of the OH–benzene adduct with O$_2$: reversibility and secondary formation of HO$_2$, Phys. Chem. Chem. Phys., 1, 5097–5107, https://doi.org/10.1039/A904887A, 1999.

Burkholder, J. B., Abbatt, J. P. D., Barnes, I., Roberts, J. M., Melamed, M. L., Ammann, M., Bertram, A. K., Cappa, C. D., Carlton, A. G., Carpenter, L. J., Crowley, J. N., Dubowski, Y., George, C., Heard, D. E., Herrmann, H., Keutsch, F. N., Kroll, J. H., McNeill, V. F., Ng, N. L., Nizkorodov, S. A., Orlando, J. J., Percival, C. J., Picquet-Varrault, B., Rudich, Y., Seakins, P. W., Surratt, J. D., Tanimoto, H., Thornton, J. A., Tong, Z., Tyndall, G. S., Wahner, A., Weschler, C. J., Wilson, K. R., and Ziemann, P. J.: The essential role for laboratory studies in at-

mospheric chemistry, Environ. Sci. Technol., 51, 2519–2528, https://doi.org/10.1021/acs.est.6b04947, 2017.

Burkholder, J. B., Sander, S. P., Abbatt, J. P. D., Barker, J. R., Huie, R. E., Kolb, C. E., Kurylo, M. J., Orkin, V. L., Wilmouth, D. M., and Wine, P. H.: Chemical kinetics and photochemical data for use in atmospheric studies–evaluation number 19, Nasa panel for data evaluation technical report, 19-5, 1–1610, https://jpldataeval.jpl.nasa.gov/pdf/NASA-JPLEvaluation19-5.pdf (last access: 25 October 2024), 2020.

Buszek, R. J., Francisco, J. S., and Anglada, J. M.: Water effects on atmospheric reactions, Int. Rev. Phys. Chem., 30, 335–369, https://doi.org/10.1080/0144235X.2011.634128, 2011.

Chao, W., Jr-Min Lin, J., Takahashi, K., Tomas, A., Yu, L., Kajii, Y., Batut, S., Schoemaecker, C., and Fittschen, C.: Water vapor does not catalyze the reaction between methanol and OH radicals, Angew. Chem. Int. Ed., 58, 5013–5017, https://doi.org/10.1002/anie.201900711, 2019.

Christensen, L. E., Okumura, M., Sander, S. P., Friedl, R. R., Miller, C. E., and Sloan, J. J.: Measurements of the rate constant of HO$_2$ + NO$_2$ + N$_2$ → HO$_2$NO$_2$ + N$_2$ using near-infrared wavelength-modulation spectroscopy and UV−visible absorption spectroscopy, J. Phys. Chem. A, 108, 80–91, https://doi.org/10.1021/jp035905o, 2004.

Cox, R. A. and Burrows, J. P.: Kinetics and mechanism of the disproportionation of HO$_2$ in the gas phase, J. Chem. Phys., 20, 2560–2588, https://doi.org/10.1021/j100483a002, 1979.

Ehhalt, D. H.: Photooxidation of trace gases in the troposphere, Phys. Chem. Chem. Phys., 1, 5401–5408, https://doi.org/10.1039/a905097c, 1999.

Ervens, B., Rickard, A., Aumont, B., Carter, W. P. L., McGillen, M., Mellouki, A., Orlando, J., Picquet-Varrault, B., Seakins, P., Stockwell, W. R., Vereecken, L., and Wallington, T. J.: Opinion: Challenges and needs of tropospheric chemical mechanism development, Atmos. Chem. Phys., 24, 13317–13339, https://doi.org/10.5194/acp-24-13317-2024, 2024.

Fiore, A. M., Mickley, L. J., Zhu, Q., and Baublitz, C. B.: Climate and tropospheric oxidizing capacity, Annu. Rev. Earth Planet. Sci. 52, 321–349, https://doi.org/10.1146/annurev-earth-032320-090307, 2024.

Fuchs, H., Bohn, B., Hofzumahaus, A., Holland, F., Lu, K. D., Nehr, S., Rohrer, F., and Wahner, A.: Detection of HO$_2$ by laser-induced fluorescence: calibration and interferences from RO$_2$ radicals, Atmos. Meas. Tech., 4, 1209–1225, https://doi.org/10.5194/amt-4-1209-2011, 2011.

Fuchs, H., Hofzumahaus, A., Rohrer, F., Bohn, B., Brauers, T., Dorn, H.-P., Häseler, R., Holland, F., Kaminski, M., Li, X., Lu, K., Nehr, S., Tillmann, R., Wegener, R., and Wahner, A.: Experimental evidence for efficient hydroxyl radical regeneration in isoprene oxidation, Nat. Geosci., 6, 1023–1026, https://doi.org/10.1038/NGEO1964, 2013.

Fuchs, H., Acir, I.-H., Bohn, B., Brauers, T., Dorn, H.-P., Häseler, R., Hofzumahaus, A., Holland, F., Kaminski, M., Li, X., Lu, K., Lutz, A., Nehr, S., Rohrer, F., Tillmann, R., Wegener, R., and Wahner, A.: OH regeneration from methacrolein oxidation investigated in the atmosphere simulation chamber SAPHIR, Atmos. Chem. Phys., 14, 7895–7908, https://doi.org/10.5194/acp-14-7895-2014, 2014.

Fulle, D., Hamann, H. F., Hippler, H., and Troe, J.: High pressure range of addition reactions of HO. II. Temperature and pressure

dependence of the reaction HO + CO ↔ HOCO → H + CO$_2$, J. Chem. Phys., 105, 983–1000, https://doi.org/10.1063/1.471991, 1996.

Gierczak, T., Jiménez, E., Riffault, V., Burkholder, J. B., and Ravishankara, A. R.: Thermal decomposition of HO$_2$NO$_2$ (peroxynitric acid, PNA): Rate coefficient and determination of the enthalpy of formation, J. Phys. Chem. A, 109, 586–596, https://doi.org/10.1021/jp046632f, 2005.

Griffith, S. M., Hansen, R. F., Dusanter, S., Michoud, V., Gilman, J. B., Kuster, W. C., Veres, P. R., Graus, M., de Gouw, J. A., Roberts, J., Young, C., Washenfelder, R., Brown, S. S., Thalman, R., Waxman, E., Volkamer, R., Tsai, C., Stutz, J., Flynn, J. H., Grossberg, N., Lefer, B., Alvarez, S. L., Rappenglueck, B., Mielke, L. H., Osthoff, H. D., and Stevens, P. S.: Measurements of hydroxyl and hydroperoxy radicals during CalNex-LA: Model comparisons and radical budgets, J. Geophys. Res., 121, 4211–4232, https://doi.org/10.1002/2015JD024358, 2016.

Heard, D. E. and Henderson, D. A.: Quenching of OH(A$^2\sum^+$, $\nu' = 0$) several collision partners between 200 and 344 K. Cross-section measurements and model comparisons, Phys. Chem. Chem. Phys., 2, 67–72, 2000.

Hofzumahaus, A. and Stuhl, F.: Rate constant of the reaction HO + CO in the presence of N$_2$ and O$_2$, Ber. Bunsenges. Phys. Chem., 88, 557–561, https://doi.org/10.1002/bbpc.19840880612, 1984.

Hofzumahaus, A., Rohrer, F., Lu, K., Bohn, B., Brauers, T., Chang, C.-C., Fuchs, H., Holland, F., Kita, K., Kondo, Y., Li, X., Lou, S., Shao, M., Zeng, L., Wahner, A., and Zhang, Y.: Amplified trace gas removal in the troposphere, Science, 324, 1702–1704, https://doi.org/10.1126/science.1164566, 2009.

Hynes, A. J., Wine, P. H., and Ravishankara, A. R.: Kinetics of the OH + CO reaction under atmospheric conditions, J. Geophys. Res., 91, 11815–11820, https://doi.org/10.1029/JD091iD11p11815, 1986.

IUPAC: Task Group on Atmospheric Chemical Kinetic Data Evaluation, Data sheets for gas phase reactions of NO$_x$ species, Data Sheet I.A3.46 NOx16, https://iupac.aeris-data.fr/ (last access: 24 October 2024), 2017a.

IUPAC: Task Group on Atmospheric Chemical Kinetic Data Evaluation, Data sheets for gas phase reactions of NOx species, Data Sheet I.A3.42 NOx12, https://iupac.aeris-data.fr/ (last access: 24 October 2024), 2017b.

IUPAC: Task Group on Atmospheric Chemical Kinetic Data Evaluation, Data sheets for gas phase reactions of NO$_x$ species, Data Sheet I.A3.43 NOx13, https://iupac.aeris-data.fr/ (last access: 24 October 2024), 2017c.

Ivanov, A. V., Trakhtenberg, S., Bertram, A. K., Gershenzon, Y. M., and Molina, M. J.: OH, HO$_2$, and ozone gaseous diffusion coefficients, J. Phys. Chem. A, 111, 1632–1637, https://doi.org/10.1021/jp066558w, 2007.

Johnson, C. J., Otto, R., and Continetti, R. E.: Spectroscopy and dynamics of the HOCO radical: insights into the OH + CO → H + CO$_2$ reaction, Phys. Chem. Chem. Phys., 16, 19091–19105, https://doi.org/10.1039/C4CP02593H, 2014.

Kanno, N., Tonokura, K., Tezaki, A., and Koshi, M.: Water dependence of the HO$_2$ self reaction: Kinetics of the HO$_2$–HO$_2$ complex, J. Phys. Chem. A, 109, 3153–3158, https://doi.org/10.1021/jp044592+, 2005.

Khan, M. A. H., Cooke, M. C., Utembe, S. R., Archibald, A. T., Derwent, R. G., Jenkin, M. E., Morris, W. C., South, N.,

Hansen, J. C., Francisco, J. S., Percival, C. J., and Shallcross, D. E.: Global analysis of peroxy radicals and peroxy radical-water complexation using the STOCHEM-CRI global chemistry and transport model, Atmos. Environ., 106, 278–287, https://doi.org/10.1016/j.atmosenv.2015.02.020, 2015.

Kim, S., Huey, L. G., Stickel, R. E., Tanner, D. J., Crawford, J. H., Olson, J. R., Chen, G., Brune, W. H., Ren, X., Lesher, R., Wooldridge, P. J., Bertram, T. H., Perring, A., Cohen, R. C., Lefer, B. L., Shetter, R. E., Avery, M., Diskin, G., and Sokolik, I.: Measurement of HO$_2$NO$_2$ in the free troposphere during the Intercontinental Chemical Transport Experiment–North America 2004, J. Geophys. Res., 112, D12S01, https://doi.org/10.1029/2006JD007676, 2007.

Kircher, C. C. and Sander, S. P.: Kinetics and mechanism of HO$_2$ and DO$_2$ disproportionations, J. Phys. Chem., 88, 2082–2091, https://doi.org/10.1021/j150654a029, 1984.

Kleffmann, J., Gavriloaiei, T., Hofzumahaus, A., Holland, F., Koppmann, R., Rupp, L., Schlosser, E., Siese, M., and Wahner, A.: Daytime formation of nitrous acid: A major source of OH radicals in a forest, Geophys. Res. Lett., 32, L05818, https://doi.org/10.1029/2005GL022524, 2005.

Kovacs, T. A. and Brune, W. H.: Total OH loss rate measurement, J. Atmos. Chem., 39, 105–122, 2001.

Kurylo, M. J. and Ouellette, P. A.: Pressure dependence of the rate constant for the reaction HO$_2$ + NO$_2$ + M → HO$_2$NO$_2$ + M (M = N$_2$, O$_2$) at 298 K, J. Phys. Chem., 90, 441–444, https://doi.org/10.1021/j100275a018, 1986.

Liessmann, M., Miller, Y., Gerber, B., and B., A.: Reaction of OH and NO at Low Temperatures in the Presence of Water: the Role of Clusters, Zeitschrift für physikalische Chemie, 225, 1129–1144, https://doi.org/10.1524/zpch.2011.0181, 2011.

Lii, R.-R., Sauer, Myran C., J., and Gordon, S.: Temperature dependence of the gas-phase self-reaction of hydroperoxo in the presence of water, J. Phys. Chem., 85, 2833–2834, https://doi.org/10.1021/j150619a027, 1981.

Liu, Y. and Sander, S. P.: Rate constant for the OH + CO reaction at low temperatures, J. Chem. Phys. A, 119, 10060–10066, https://doi.org/10.1021/acs.jpca.5b07220, 2015.

Lou, S., Holland, F., Rohrer, F., Lu, K., Bohn, B., Brauers, T., Chang, C. C., Fuchs, H., Häseler, R., Kita, K., Kondo, Y., Li, X., Shao, M., Zeng, L., Wahner, A., Zhang, Y., Wang, W., and Hofzumahaus, A.: Atmospheric OH reactivities in the Pearl River Delta – China in summer 2006: measurement and model results, Atmos. Chem. Phys., 10, 11243–11260, https://doi.org/10.5194/acp-10-11243-2010, 2010.

Martinez, M., Harder, H., Kovacs, T. A., Simpas, J. B., Bassis, J., Lesher, R., Brune, W. H., Frost, G. J., Williams, E. J., Stroud, C. A., Jobson, B. T., Roberts, J. M., Hall, S. R., Shetter, R. E., Wert, B., Fried, A., Alicke, B., Stutz, J., Young, V. L., White, A. B., and Zamora, R. J.: OH and HO$_2$ concentrations, sources, and loss rates during the Southern Oxidants Study in Nashville, Tennessee, summer 1999, J. Geophys. Res., 108, 4617, https://doi.org/10.1029/2003JD003551, 2003.

McCabe, D. C., Gierczak, T., Talukdar, R. K., and Ravishankara, A. R.: Kinetics of the reaction OH + CO under atmospheric conditions, Geophys. Res. Lett., 28, 3135–3138, https://doi.org/10.1029/2000GL012719, 2001.

McKee, K., Blitz, M. A., Shannon, R. J., and Pilling, M. J.: HO$_2$ + NO$_2$: Kinetics, Thermochemistry, and evidence for a bi-

molecular product channel, J. Phys. Chem. A, 126, 7514–7522, https://doi.org/10.1021/acs.jpca.2c04601, 2022.

Miyazaki, K., Nakashima, Y., Schoemaecker, C., Fittschen, C., and Kajii, Y.: Note: A laser-flash photolysis and laser-induced fluorescence detection technique for measuring total HO$_2$ reactivity in ambient air, Rev. Sci. Instrum., 84, 076106, https://doi.org/10.1063/1.4812634, 2013.

Miyoshi, A., Matsui, H., and Washida, N.: Detection and reactions of the HOCO radical in gas phase, J. Chem. Phys., 100, 3532–3539, https://doi.org/10.1063/1.466395, 1994.

Mollner, A. K., Valluvadasan, S., Feng, L., Sprague, M. K., Okumura, M., Milligan, D. B., Bloss, W. J., Sander, S. P., Martien, P. T., Harley, R. A., McCoy, A. B., and Carter, W. P. L.: Rate of gas phase association of hydroxyl radical and nitrogen dioxide, Science, 330, 646–649, https://doi.org/10.1126/science.1193030, 2010.

Nakashima, Y., Tsurumaru, H., Imamura, T., Bejan, I., Wenger, J. C., and Kajii, Y.: Total OH reactivity measurements in laboratory studies of the photooxidation of isoprene, Atmos. Environ., 62, 243–247, https://doi.org/10.1016/j.atmosenv.2012.08.033, 2012.

Nehr, S., Bohn, B., Fuchs, H., Hofzumahaus, A., and Wahner, A.: HO$_2$ formation from the OH + benzene reaction in the presence of O$_2$, Phys. Chem. Chem. Phys., 13, 10699–10708, https://doi.org/10.1039/C1CP20334G, 2011.

Nehr, S., Bohn, B., and Wahner, A.: Prompt HO$_2$ formation following the reaction of OH with aromatic compounds under atmospheric conditions, J. Phys. Chem. A, 116, 6015–6026, https://doi.org/10.1021/jp210946y, 2012.

Newsome, B. and Evans, M.: Impact of uncertainties in inorganic chemical rate constants on tropospheric composition and ozone radiative forcing, Atmos. Chem. Phys., 17, 14333–14352, https://doi.org/10.5194/acp-17-14333-2017, 2017.

Okabe, H.: Photochemistry of small molecules, John Wiley and Sons, https://doi.org/10.1002/nadc.19790270512, 1978.

Overend, R., Paraskevopoulos, G., and Black, C.: Rates of OH radical reactions. II. The combination reaction OH + NO + M, J. Chem. Phys., 64, 4149–4154, https://doi.org/10.1063/1.431984, 1976.

Paraskevopoulos, G. and Irwin, R. S.: The pressure dependence of the rate constant of the reaction of OH radicals with CO, J. Phys. Chem., 80, 259–266, https://doi.org/10.1063/1.446488, 1984.

Sadanaga, Y., Yoshino, A., Kato, S., Watanaba, K., Miyakawa, Y., Hayashi, I., and Kajii, Y.: The importance of NO$_2$ and volatile organic compounds in the urban air from the viewpoint of the OH reactivity, Geophys. Res. Lett., 31, L08102, https://doi.org/10.1029/2004GL019661, 2004a.

Sadanaga, Y., Yoshino, A., Watanaba, K., Yoshioka, A., Wakazono, Y., Kanaya, Y., and Kajii, Y.: Development of a measurement system of peroxy radicals using a chemical amplification/laser-induced fluorescence technique, Rev. Sci. Instrum., 75, 864–872, https://doi.org/10.1063/1.1666985, 2004b.

Sadanaga, Y., Kondo, S., Hashimoto, K., and Kajii, Y.: Measurement of the rate coefficient for the OH + NO$_2$ reaction under the atmospheric pressure: Its humidity dependence, Chem. Phys. Lett., 419, 474–478, https://doi.org/10.1016/j.cplett.2005.12.026, 2006.

Sander, S. P. and Peterson, M. E.: Kinetics of the reaction HO$_2$ + NO$_2$ + M → HO$_2$NO$_2$ + M, J. Phys. Chem., 88, 1566–1571, https://doi.org/10.1021/j150652a025, 1984.

Sharkey, P., Sims, I. R., Smith, I. W. M., Bocherel, P., and Rowe, B. R.: Pressure and temperature dependence of the rate constants for the association reaction of OH radicals with NO between 301 and 23 K, J. Chem. Soc. Faraday Trans., 90, 3609–3616, https://doi.org/10.1039/FT9949003609, 1994.

Sheps, L. and Au, K.: New instrument for time-resolved OH and HO$_2$ quantification in high-pressure laboratory kinetics studies, J. Phys. Chem. A, 128, 3916–3925, https://doi.org/10.1021/acs.jpca.4c00994, 2024.

Smith, I. W. M. and Zellner, R.: Rate measurements of reactions of OH by resonance absorption. Part 2. Reactions of OH with CO, C$_2$H$_4$ and C$_2$H$_2$, J. Chem. Soc., Faraday Trans. 2, 69, 1617–1627, https://doi.org/10.1039/F29736901617, 1973.

Speak, T. H., Blitz, M. A., Stone, D., and Seakins, P. W.: A new instrument for time-resolved measurement of HO$_2$ radicals, Atmos. Meas. Tech., 13, 839–852, https://doi.org/10.5194/amt-13-839-2020, 2020.

Stone, D., Blitz, M., Ingham, T., Onel, L., Medeiros, D. J., and Seakins, P. W.: An instrument to measure fast gas phase radical kinetics at high temperatures and pressures, Rev. Sci. Instr., 87, 054102, https://doi.org/10.1063/1.4950906, 2016.

Strotkamp, M., Munk, A., Jungbluth, B., Dahlhoff, K., Jansen, P., Broch, S., Gomm, S., Bachner, M., Fuchs, H., Holland, F., and Hofzumahaus, A.: Design of a rugged 308 nm tunable UV laser for airborne LIF measurements on top of Zeppelin NT, Solid State Lasers Xxii: Technology and Devices, Proceedings of SPIE, 8599, 85990L, https://doi.org/10.1117/12.2000408, 2013.

Sun, W., Lelieveld, J., and Crowley, J. N.: Rate coefficients for OH + NO(+N$_2$) in the fall-off regime and the impact of water vapor, J. Phys. Chem. A, 126, 3863–3872, https://doi.org/10.1021/acs.jpca.2c02369, 2022.

Troe, J.: Theory of thermal unimolecular reactions in the fall-off range. I, Strong collision rate constants, Ber. Bunsen Phys. Chem., 87, 161–169, https://doi.org/10.1002/bbpc.19830870217, 1983.

Vandaele, A. C., Hermans, C., Simon, P. C., Carleer, M., Colin, R., Fally, S., M'erienne, M. F., Jenouvrier, A., and Coquart, B.: Measurements of the NO$_2$ absorption cross-section from 42 000 cm^{-1} to 10 000 cm^{-1} (238–1000 nm) at 220 K and 294 K, J. Quant. Spe. Rad. Trans., 59, 171–184, https://doi.org/10.1016/S0022-4073(97)00168-4, 1998.

Whalley, L. K., Edwards, P. M., Furneaux, K. L., Goddard, A., Ingham, T., Evans, M. J., Stone, D., Hopkins, J. R., Jones, C. E., Karunaharan, A., Lee, J. D., Lewis, A. C., Monks, P. S., Moller, S. J., and Heard, D. E.: Quantifying the magnitude of a missing hydroxyl radical source in a tropical rainforest, Atmos. Chem. Phys., 11, 7223–7233, https://doi.org/10.5194/acp-11-7223-2011, 2011.

Winiberg, F. A. F., Zuraski, K., Liu, Y., Sander, S. P., and Percival, C. J.: Pressure and temperatured dependencies of rate coefficients for the reaction OH+NO$_2$+M → products, J. Phys. Chem. A, 124, 10121–10131, https://doi.org/10.1021/acs.jpca.0c08920, 2020.

Yang, Y., Shao, M., Wang, X., Nölscher, A. C., Kessel, S., Guenther, A., and Williams, J.: Towards a quantitative understanding

of total OH reactivity: A review, Atmos. Environ., 134, 147–161, https://doi.org/10.1016/j.atmosenv.2016.03.010, 2016.

Zellweger, C., Steinbacher, M., and Buchmann, B.: Evaluation of new laser spectrometer techniques for in-situ carbon monoxide measurements, Atmos. Meas. Tech., 5, 2555–2567, https://doi.org/10.5194/amt-5-2555-2012, 2012.

Zhou, J., Murano, K., Kohno, N., Sakamoto, Y., and Kajii, Y.: Real-time quantification of the total HO$_2$ reactivity of ambient air and HO$_2$ uptake kinetics onto ambient aerosols in Kyoto (Japan), Atmos. Environ., 223, 117189, https://doi.org/10.1016/j.atmosenv.2019.117189, 2019.